THE RADIATIVE EFFECT OF AEROSOLS FROM BIOMASS BURNING ON THE TRANSITION FROM DRY TO WET SEASON OVER THE AMAZON AS TESTED BY A REGIONAL CLIMATE MODEL

A Thesis
Presented to
The Academic Faculty

by

Yan Zhang

In Partial Fulfillment
of the Requirements for the Degree
Doctor of Philosophy in the
School of Earth and Atmospheric Sciences

Georgia Institute of Technology

December, 2008

THE RADIATIVE EFFECT OF AEROSOLS FROM BIOMASS BURNING ON THE TRANSITION FROM DRY TO WET SEASON OVER THE AMAZON AS TESTED BY A REGIONAL CLIMATE MODEL

Approved by:

Dr. Rong Fu, Advisor
School of Earth and Atmospheric Sciences
Georgia Institute of Technology

Dr. Athanasios Nenes
School of Earth and Atmospheric Sciences
Georgia Institute of Technology

Dr. Robert E. Dickinson
School of Earth and Atmospheric Sciences
Georgia Institute of Technology

Dr. Hongbin Yu
Goddard Earth Science and Technology Center
University of Maryland Baltimore County

Dr. Peter Webster
School of Earth and Atmospheric Sciences
Georgia Institute of Technology

Date Approved: July 28, 2008

ACKNOWLEDGEMENTS

I acknowledge the immeasurable contribution of Prof. Rong Fu to this study and to my graduate experience. I express appreciation for the help of Prof. Robert Dickinson regarding the land model. This dissertation would be impossible without their continuous encouragement and support. I am grateful for the support, help and discussions with Drs. Hongbin Yu (University of Maryland Baltimore County and NASA GSFC) and Robinson Negron Juarez (Tulent University). I thank Profs. Robert Dickinson, Peter Webster, Thanos Nenes, and Dr. Hongbin Yu for reading this thesis and providing valuable feedback. Finally, my graduate studies would not be nearly as enjoyable without the encouragement and help from with my current and past group members Drs. Yan Huang, Qing Liu, Hui Wang (NOAA), Katia Fernandes, Wenhong Li, Paola Arias, Liming Zhou (NSF), Yuhong Tian, Huiling Gao (University of Washington), Mi Zhou (NOAA), M. Shaikh, Yanping He , and Willis Shem (UGA).

This work would not be possible without unconditional love and support from my husband Xiaoshan Xu and my parents.

TABLE OF CONTENTS

LIST OF TABLES

Page

LIST OF FIGURES

SUMMARY

I have carried out a set of ensemble simulations of a regional climate model with observed radiative forcing for smoke aerosols over the Amazon to investigate the radiative effects of aerosols on clouds, rainfall, and circulation from dry to wet season. I first modified the land surface scheme such that the modeled daily mean and diurnal cycle of the surface sensible and latent heat fluxes are much more realistic over the Amazon rainforest. The results of the ensemble simulations suggest that the radiative effect of the smoke aerosols can reduce daytime surface radiative and sensible fluxes, the depth and instability of the planetary boundary layer (PBL), consequently the clouds in the lower troposphere in early afternoon in the smoke center, where the aerosols optical depth, AOD, exceeds 0.3. The aerosol radiative forcing also appears to weaken moisture transport into the smoke center and increase moisture transport and cloudiness in the region upwind to the smoke center, namely, the northern Amazon. In particular, the absorption of solar radiation by smoke aerosols reduces cloudiness in early afternoon. This reduction of cloud partially compensates for the reduction of surface solar flux by aerosol scattering, shifting the strongest changes of surface flux and the PBL to late morning. The reduction of net solar radiation at the surface by smoke is locally largely compensated by reduction of surface sensible flux; with reduction of latent flux only about 30% as large. This is because, in model, transpiration of the forest canopy response favorably to the reduced leaf temperature by aerosols at local noon, which compensates the reduction of evapotranspiration (ET) in morning and later afternoon. Strong aerosol absorption in the top 1 km of the aerosol layer stabilizes the 2 to 3 km

layer immediately above the daytime PBL and consequently cloudiness decreases. This reduced surface solar flux and more stable lapse rate at the top of the PBL stabilize the lower troposphere, leading to a higher surface pressure in the smoke center and so weakens the southward surface pressure gradient between northern and southern Amazonia that drives the northerly moisture transport to southern Amazonia. Consequently, an anomalous moisture divergence appears in the smoke center in southern Amazonia. While these changes can reduce clouds in the lower troposphere, they do not appear to reduce rainfall in the smoke center, presumably because the atmosphere is mostly already too stable to rain.

In the northwestern Amazon, anomalous wind convergence over the equatorial western Amazon occurs to compensate the anomalous wind divergence in the southern Amazon, leading to an increase of both clouds and rainfall in that region. The increased atmospheric thermodynamic stability in Southern Amazonia also appears to block synoptic cyclonic activities propagated from extratropical South America, leading to an increased synoptic cyclonic activities and rainfall in southern Brazil, Paraguay and northern Argentina. Evidently, the dynamic response of the monsoon circulation plays a major role in determining the pattern of rainfall change induced by the radiative effect of aerosols.

CHAPTER 1

GOAL AND MOTIVATION

During the transition from the wet to dry season (August – October) in the Amazon basin, biomass burning emits a large amounts of absorbing aerosols into the atmosphere. As shown in Figure 1.1 (top panel), the aerosol optical depth in the dry season is several times larger than that in the wet season (also Andreae et al., 2002; Schafer et al., 2008). Satellite data have also suggested a statistically significant increasing tendency of biomass burning smoke in recent years (Koren et al., 2007; and figure 1.1 middle and bottom panels). Smoke aerosols can substantially influence radiation budget, directly through scattering and absorbing solar radiation, and indirectly through altering fractional coverage and microphysical and optical properties of clouds. The onset of rainy season in the Amazon provides much of the diabatic heating needed for establishing the South American Monsoon circulation (Lenters and Cook, 1999). Fu et al. (1999) have shown that the atmosphere over the Amazon is very close to neutral to moist convection. Thus, a surface temperature change of a few degrees or surface humidity changes of 1 g/kg is responsible for the seasonal change of convection over the Amazon. Therefore, changes of clouds and rainfall in Amazon are sensitive to small changes, comparable to those induced by biomass burning aerosols. In addition, the monsoon transition is initiated by an increase of surface solar flux, which in turn, increases surface latent and sensible fluxes (Li and Fu 2004). The timing of the peak biomass at the monsoon onset raises a question as to whether the biomass burning aerosols influence rainfall in the transition between dry to wet season. Very few previous

studies have explored the impact of biomass burning aerosols on the South American monsoon, and virtually none of them address the mechanisms through which the biomass burning aerosols might affect the monsoon transition. This study aims to address these issues.

Liu et al. (2005), was the first to suggest that biomass burning aerosols may influence the development of South American monsoon. *Liu* (2005) used a regional climate model to simulate atmospheric response and feedback to radiative forcing from smoke aerosols during dry to wet transition season. These studies indicated the potential importance of the biomass burning aerosol radiative effect on monsoon circulation, albeit with several limitations. For example, the modeled land surface was too dry during the transition season, when compared to the observations, raising a question as to whether the transition process was adequately represented in those simulations. The experiments were forced by spatially uniform aerosols and only a single pair of simulation with and without aerosols was performed. Thus, whether the effect of aerosol forcing, as represented by the difference between control and aerosol simulations, was significant or not remains unknown. The diurnal cycle of the land surface fluxes and the planetary boundary layer plays a central role in determining the formation of clouds and convection over land, especially in South America (Fu et al. 1999, Betts and Jacobs 2002), but their roles in determining aerosols impact on monsoon were not addressed in Liu (2005). Finally, the mechanisms through which biomass burning aerosols influence monsoon transition for South America were not examined.

In this study, we address these issues through ensemble simulations of a regional climate model. The influences of smoke aerosols on the diurnal changes of the surface

fluxes, clouds, and the PBL height are examined in detail. This study also uses the improved surface climate conditions in the regional climate model and spatially varying aerosol distributions. We also explore whether or not smoke aerosols can alter the processes which are key to monsoon circulation transition in the Amazon basin. In doing so, we aim to clarify the mechanisms through which biomass burning aerosols influence the land-atmosphere interaction and large-scale rainfall patterns.

Chapter 2 provides a brief summary of aerosol impacts on radiation, cloud, and the hydrological cycle, and the key characteristics of the South American Monsoon system. Chapter 3 describes the regional model, experiment design and improvement in the modeled surface fluxes. Chapter 4 shows model results of influences of biomass burning aerosols on diurnal cycle of surface fluxes, the PBL, and clouds in the lower troposphere. Chapter 5 addresses the impact of biomass burning aerosols on rainfall and monsoon circulation transition. Chapter 6 summarizes conclusions from this study and discusses future work to address the aerosol-monsoon connections.

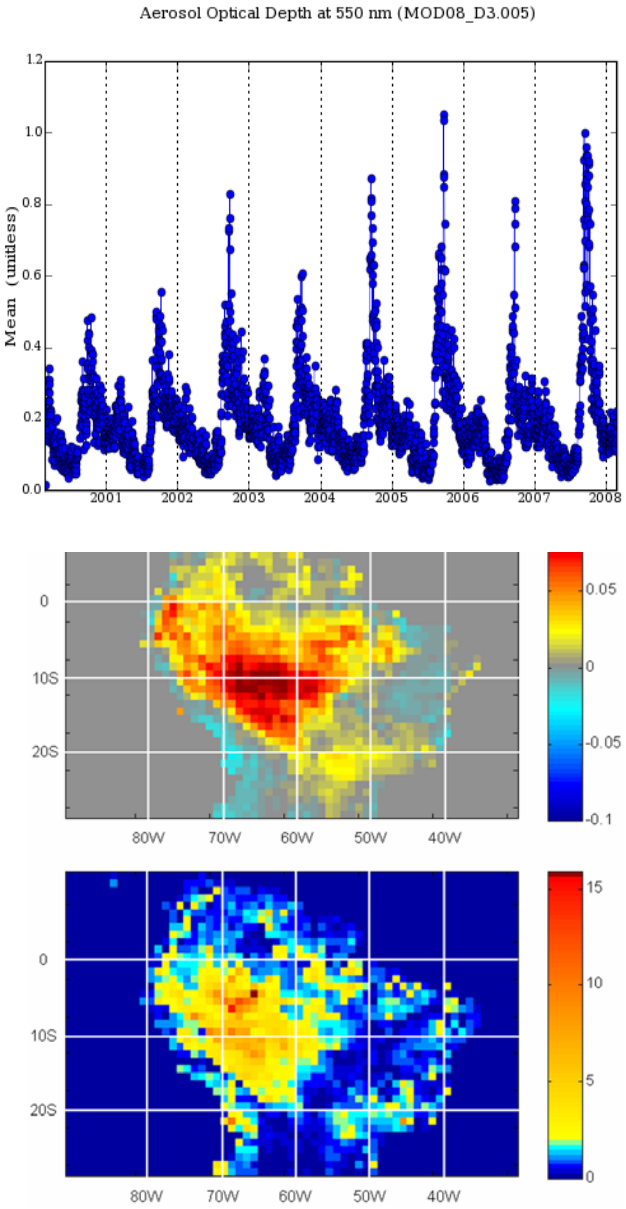

Figure 1.1: (top) 8-year average aerosol optical depth over Amazon (35-75W, 20S-5N) (courtesy of NASA Giovanni), (middle) Slopes of the trend regression line for each 1 degree square for the six year period (2000–2005). Units are in AOD per season. (bottom) The t-statistic for the student's t-test of the calculated trends in each 1 degree square. The color bar has been stretched in such a way that yellows and oranges denote significance at the 95% confidence level ($t > 2.7765$) and light blue denotes significance at the 90% confidence level ($t > 2.1318$) (From: Koren et al., 2007).

CHAPTER 2

BACKGROUND

2.1 Aerosol effects on atmospheric radiative forcing and hydrological cycle

Biomass burning is one of the major sources of atmospheric aerosols in the tropics. Most of this activity takes place in the monsoon regions in Africa, Southeast Asia, and South America, and is coupled with seasonal and interannual climate variability of the monsoon systems. The main components of biomass burning aerosols are carbonaceous aerosols which include organic carbon and black carbon (the main source of absorbing aerosols). The global emission of organic carbon and black carbon from biomass burning has been estimated as 45 ~ 80 Tg/yr and 6 ~ 9 Tg/yr, respectively (IPCC, 2001). As for aerosols in general, the biomass burning aerosols can influence the climate system through altering the radiative energy budget of the earth's climate system, and through altering the dynamic and thermodynamic structure of the atmospheric circulation. Most research has been focused on aerosols impact on the Earth's radiation field, although the impact of aerosols on large-scale monsoon circulation has begun to receive increased attention (Lau et al., 2008).

Similar to other aerosols from other sources, aerosols from biomass burning can influence the climate system in a variety of ways. Aerosols can scatter and absorb radiation, thus altering radiative fluxes in the atmosphere and at the earth's surface (McCormick and Ludwig, 1967; Charlson and Pilat, 1969; Coakley et al., 1983). This is referred to as the "direct" effect. Aerosols acting as cloud condensation nuclei (CCN) and ice nuclei (IN) can affect cloud microphysical and radiative properties (Twomey et al.,

1977; Albrecht, 1989). Other things being equal, an increase of aerosols can increase the number concentration of cloud droplets and decrease cloud droplet size, consequently increasing the brightness of the cloud and thus altering cloud structure and life time. This is referred to as the 'indirect effect'. Aerosols can also modify the atmospheric lapse rate and surface heat and water fluxes, which change the thermodynamic stability and therefore circulation of the atmosphere. These changes can affect cloudiness, precipitation, and aerosol distribution, which further changes the radiative balance of the climate system. This is referred to as the 'semi-direct effect'. The direct aerosol effect is relatively well understood, although those effects are complicated for aerosols that are over or under clouds. The aerosol semi-direct and indirect effects are still not well understood.

Key parameters for determining the aerosol direct radiative forcing are the aerosol absorption and scattering properties (the single scattering albedo, ω_o, and the scattering phase function). These parameters depend on wavelength, aerosol composition and shape, mixture state in the atmosphere, the distribution of the aerosols relative to clouds, underlying surface properties (e.g., surface reflectance and albedo), and solar zenith angle (e.g., Haywood, and Boucher, 2000; Penner et al., 2001; Ramaswamy et al., 2001). The Intergovernmental Panel on Climate Change (IPCC) Fourth Assessment Report (AR4) in 2007 reported that the total direct aerosol radiative forcing from models and observations is estimated to be +0.5 (±0.4) W m^{-2} at the top of the atmosphere (TOA), with a medium-low level of scientific understanding. Within this total direct aerosol radiative forcing, biomass burning aerosol is estimated to be +0.03 (±0.12) W m^{-2}, with the uncertainty greater than the mean value. IPCC Third Assessment Report (TAR) in 2001 reported a -

0.2 W m^{-2} radiative forcing from biomass burning aerosol which is estimated with a roughly -0.4 W m^{-2} from the organic carbon which scatters the solar radiation, and +0.2 W m^{-2} from the black carbon which would absorb the solar radiation. This sign difference between AR4 and TAR is because of the uncontrolled emission of biomass burning aerosol and the improvement of the models presentation of physical and optical properties as well as the vertical profile of biomass burning aerosols which is critical in assessing the magnitude and sign of the direct radiative forcing (Myhre et al., 2003; Penner et al., 2003). Over the Amazon, the aerosol radiative forcing is much greater. Procopio et al.(2005) reported that the monthly average direct forcing of biomass burning aerosol at the TOA varied from -5 to -12 W m^{-2} and at the surface varied from -21 to -74 W m^{-2} from measurements during the dry season. Clearly the aerosol radiative forcing at surface is much greater than that at TOA because of absorption by smoke aerosols and the atmospheric heating rate increases substantially (Procopio et al., 2005; Zhou et al., 2005). This simultaneous surface cooling and atmospheric heating would stabilize the lower atmosphere and influence the evolution of the PBL, atmospheric convection and cloud formation (Hansen et al., 1997; Ackerman et al., 2000; Yu et al., 2002; Koren et al., 2004; Kaufman et al., 2006).

Most model estimations show that the contribution of aerosol direct and semi-direct effects on the TOA radiation are generally small compared with the indirect effect, ranging from +0.1 to –0.5 W m^{-2} mainly due to the variation of black carbon with respect to the cloud (Lohmann and Feichter, 2005). The simulated cloud lifetime effect in different models varies between -0.3 and -1.4 W m^{-2} (Lohmann and Feichter, 2005). The difference between model simulations is largely influenced by the empirical treatment of

relationship between aerosol mass and cloud droplet number concentration, the mechanistic relationship, or differences in the cloud microphysics scheme (Ghan et al., 1998; Jones et al., 2001; Menon et al., 2002, 2003; Penner et al., 2006). At the surface, global climate model estimates of the mean decrease in surface shortwave radiation in response to all aerosol effects vary between –1.3 and –3.3 W m^{-2} (IPCC, 2007). It is larger than the TOA radiation flux change because some aerosols like black carbon absorb solar radiation within the atmosphere compensating the aerosol scattering effect at the TOA (Jacobson, 2001; Lohmann and Feichter, 2001; Ramanathan et al., 2001; Liepert et al., 2004). Transient simulations (Roeckner et a., 1999) of coupled GCM-mixed-layer ocean simulations (Feichter et al., 2004 Liepert et al., 2004) suggest that the decrease of solar radiation at the surface resulting from the aerosol total radiative effect is more important for controlling the surface energy budget than the greenhouse-gas induced increase in surface temperature.

Currently, no general consensus has been reached as to how aerosol indirect effect changes cloud microphysical properties and whether it would increase or decrease clouds. For example, Yu et al. (2007) analyzed the relationship between smoke aerosols and warm clouds over Amazonia by using MODIS data and showed different behaviors of aerosol-cloud relationship in different years. Their work suggests that the aerosol-cloud relationship can be influenced by atmospheric structure and convective motions, in addition to changes in aerosol properties. Kaufman et al. (2005) suggest from satellite observations that the aerosol indirect effect increases cloud cover. Conversely, model results of Lohmann et al. (2006) indicate that the increase in cloud fraction with increasing AOT is dominated by changes in dynamical regimes, not by aerosol indirect

effects. Among GCM models, the simulated cloud response to aerosols behaves differently depending on details in the microphysics schemes, especially in the auto-conversion rate (Menon et al., 2002, 2003; Penner et al., 2006).

Semi-direct effects due to absorbing aerosols have been shown clearly in individual cases studies either through observations or through numerical simulations, but the underlying processes that are responsible for differences between the various studies are not clearly understood. For example, Ramanathan et al. (2005) found that convection was suppressed due to increased stability resulting from black carbon heating. Penner et al. (2003) suggested that the local change in atmospheric stability strongly depends on the altitude of the black carbon heating. Aerosol heating within cloud layers reduces cloud fractions, whereas aerosol heating above the cloud layer tends to increase cloud fractions (due to increase in entrainment at the cloud base) (Feingold, et al., 2005, Johnson et al., 2005).

The impact of aerosol on the large-scale circulation has been examined by GCMs (Feichter et al., 2004; Kristjansson et al., 2005; Takemura et al., 2005). Recent transient simulations (Held et al., 2005; Paeth and Feichter, 2006) found that a substantial cooling due to dust aerosols can cause a southward shift of the Inter-Tropical Convergence Zone (ITCZ) and the associated tropical rainfall in the northern hemisphere. Menon et al. (2002) found that absorbing aerosols induce rising motions to the south and increase subsidence to the north in India and China. Wang (2004) concluded that convection and associated precipitation are substantially enhanced by dust aerosols (as much as 15% in zonal-mean precipitation rate) in the north portion of the ITCZ and reduced (up to 23% in zonal-mean precipitation rate) in the south part of the ITCZ.

Tropical biomass burning emission occurs mostly in the monsoon region. Whether or not biomass burning aerosols can affect monsoon dynamics remains largely unknown. Recently, Lau et al. (2006) and Lau and Kim (2006) have demonstrated the importance of atmospheric heating by elevated absorbing aerosols (dust and black carbon) in spurring anomalous water cycle feedback, leading to an advance of the rainy periods and an intensification of the Indian summer monsoon.

2.2 The South American Monsoon

a. Basic Features

The conventional definition of a 'monsoon' is a seasonal reversal of large-scale circulation driven by differential heating between the continent and the ocean. The basic features of a monsoon include large scale land-sea temperature contrast; large-scale thermally direct circulation with a continental rising branch and an oceanic sinking branch; land-atmosphere interactions associated with elevated terrain and land surface conditions; surface low pressure and an upper level anticyclone; and intense low-level inflow of moisture to the continent with associated seasonal changes in precipitation (both increases and decreases).

The annual cycle of monsoon systems can be divided into two distinct phases (Webster, 1998); first, the wet-warm phase: the summer rainy season, during which warm, moist, and very disturbed winds blow inland from the warm tropical oceans; and second, the dry-cool phase: the other half of the year, during which winds bring cool and dry air across the monsoon regions from the winter continents. Aside from solar heating differences between continent and ocean driving the monsoon system, land surface

properties and processes, as well as variation of sea surface temperature of the tropical oceans are also factors which impact the development of monsoon system (Xue and Shukla, 1993, Fennessy et a., 1994, Torrence and Webster, 1998).

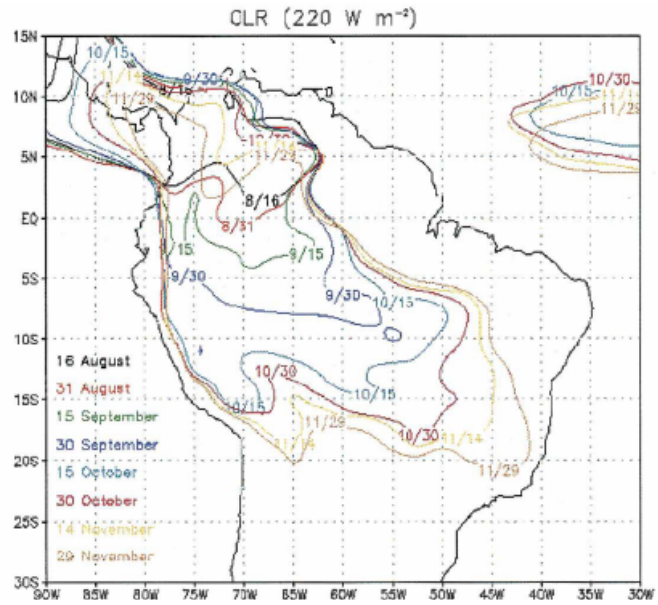

Fig. 2.2.1. Diagram indicates migration of wet season over the Amazon (From:Vera et al., 2006).

Because South America is situated in tropical region, and the seasonal temperature differences are less pronounced than in subtropical monsoon regimes, South America has not typically been considered to be a monsoon region. Using assimilation products from the data assimilation system of Goddard Earth Observing System-1 (GEOS-1) and satellite-derived rainfall, Zhou and Lau (1998), for the first time, diagnosed and confirmed the existence of summer monsoon climate over South America. The development of SAMS during austral spring is characterized by a rapid southward shift of the region of intense convection from northwestern South America to the southern Amazon Basin and Brazilian high lands (Altiplano) (Fig. 2.2.1). This monsoon

circulation transition is initialized by an increase of surface radiation and resultant increase in latent and sensible heat fluxes, which lead to destabilization of the atmospheric thermodynamic structure and an increase of the moisture transport to Amazonia (Li and Fu, 2004). The initial migration of rainfall is lead by a southward reversal of the cross-equatorial flow in the northwest corner of the South American continent (Wang and Fu, 2002). The onset across the Amazon basin lasts about one month and is followed by abundant rainfall. The onset of the wet season in central and southeastern Brazil occurs between the end of September and early October. Intraseasonal oscillations may promote rapid onset over central Brazil. By late November, deep convection covers most of central South America from the equator to 20S, but is absent over the eastern Amazon basin and northeast Brazil (Kousky 1998; Jorel et al., 1989; Marengo et al., 2001). Such rapid south migration of the rainfall is unique to the South American summer monsoon system.

b. Factors Effect on monsoon and onset of wet season

The wet-season onset date and the amount of rainfall are of importance for agriculture, hydroelectric power generation, and local ecosystems of the Amazon region. The change in the timing of onset and the end of the rainy season contributed much to the interannual variation of rainfall during the rainy season (Liebmann and Marengo, 2002). The spatial pattern and rapid shift of the wet season onset over South America has been explored by several studies (Kousky 1998; Jorel et al., 1989; Marengo et al., 2001). A recent study (Grimm et al., 2007) shows that soil moisture and surface temperature in

spring time influences the precipitation in summer monsoon season in South America. However factors control the timing of the wet season onset are still unclear.

Surface conditions and SST

It has been debated for years whether the local land surface fluxes or the more remote influences from the adjacent ocean control the rainfall and circulation of the wet season. Some suggest that the land surface fluxes control the wet season circulation pattern (Gutman and Schwedtfeger, 1965; Rao and Erdogan, 1989). Others suggest that the main source of moisture during the wet season is the transport from the Atlantic (Rao et al., 1996) and the SST in the tropical Atlantic and Pacific Oceans strongly control the precipitation over the Amazon (Namias 1972; Aceituno 1988; Fu, et al., 2001) through the direct thermal circulation of the Atlantic intertropical convergence zone (ITCZ). Fu et al. (1999) examined the atmosphere destabilization during the transition from dry to wet seasons. Their results suggested that half of the moisture in the atmospheric boundary layer during the wet season is obtained from the entrainment from the upper humid atmospheric layer in which moisture is transported from ocean.

Large scale dynamics plays a major role in the monsoon system, but the effect of surface conditions is also recognized. The effect of soil moisture on the surface fluxes and consequently on the Bowen Ratio can lead to changes in precipitation (Estela and Bergery, 2006). Li and Fu (2004) diagnosed the ECMWF Re-analysis data to show that the variation of land surface fluxes (due to, for example, land cover change) is important to the initial onset.

Cold Front and Low Level Jet

Synoptic-scale incursions of cold air from midlatitudes into the subtropics influence the regional weather and tropical convection. In South America, cold air incursion occurs year round at intervals of 1 to 2 weeks. In the winter time, these episodes produce freezing conditions from central Argentina to southern Brazil (Hamilton and Tarifa, 1978, Fortune and Kousky, 1983; Merango, 1997; Garreaud, 1999). During summer, they have less impact on the temperature and pressure, but they have been associated with enhanced convection and rainfall (Garreaud and Wallace, 1998; Libmann et al., 1999). These strong cold fronts may account for about 50% of the total summertime precipitation around 25^{o}S (Garreaud and Wallace, 1998). The mean monthly distribution of the frequency of the frontal passage between 5 ^{o}S and 20 ^{o}S is highest during the dry to wet transition season (August-September: Oliveira 1986; Machado et al., 2004). These cold fronts produce rainfall over an elongated area from the western Amazon to southeast Brazil similar to the typical geographic pattern of the rainy areas during the rapid onset of wet seasons. Li and Fu (2006) investigated whether such midlatitude cold air intrusions trigger the wet season onset by using European Centre for Medium-Range Weather Forecasts Re-Analysis (ERA-15). They suggested that the influence of cold air intrusion somehow depended on large-scale thermodynamic conditions.

The South American low level jet (SALLJ) is a strong wind observed around 20^{o}S (Bolivia near Santa Cruz de la Sierra). It is a mesoscale system related to the topography of the Andes mountains. The SALLJ is a key feature of continent's climate, transporting moisture from the Amazon basin to the higher latitudes, such as the La Plata basins (Virji 1981; Paegle et al., 1987). The jet has a diurnal cycle with a nighttime maximum that

favors increased moisture flux convergence in southeastern South America. This convergence, in turn, is associated with generalized precipitation. Vera et al. (2006) found that incursion of moisture transport from the Bolivian lowlands westward into the southern portion of the Altiplano drives convection over that region. The SALLJ maximum over Bolivia occurs year-round due to dynamical modifications produced by the Andes Mountains to the mean circulation (Byerle and Paegle 2002; Campetella and Vera, 2002). It produces seasonal rainfall over southeast of South America, around 20^{o}S, and is not characterized by a distinct warm rainy season. This region is highly sensitive to the natural climate variability, such as ENSO. For example, warm ENSO events induce positive rainfall anomalies over the region (Ropelewski and Halpert 1987). This precipitation regime covers approximately northeastern Argentina, Paraguay, southern Brazil, and parts of Uruguay.

CHAPTER 3

REGIONAL CLIMATE MODEL (REGCM3)

3.1 Model Description

Climate models are the primary tools that help scientists understanding the processes that govern the climate system. The recent years development of computer technique makes it easier to store climatic data and makes it faster to model perform. These make climate models more powerful to study variety of topics, including climate change, prediction, and variability. The idea that limited area models could be used for regional climate studies was original proposed by Dickinson et al. (1989) and Giorgi (1990). This idea was based on the concept of high-resolution limited area model forced by large-scale meteorological fields from general circulation model (GCM) as initial and boundary conditions. Using such limited area model, with its high resolutions, we can capture the topography feature of the region, such as mountains or basins, which is very important to the regional weather and climate.

The numerical model applied to this study is the Abdus Salam Institute for Theoretical Physics Regional Climate Model, version 3 (RegCM3) (Pal et al., 2000). RegCM3 is the third generation of a modeling framework originally described in Giorgi and Bates (1989) and Dickinson et al. (1989; RegCM1), then upgraded by Giorgi et al (1993a, b; RegCM2) and Giorgi and Mearns (1999; RegCM2.5).

In RegCM3, the dynamic core of RegCM3 is based on the hydrostatic version of the fifth-generation Pennsylvania State University-National Center for Atmospheric

Research (PSU-NCAR) mesoscale Model (MM5) (Grell at al., 19940), with the terrin-following sigma (σ) pressure vertical coordinate, which is defined as:

$$\sigma = \frac{p - p_t}{p_s - p_t} \tag{3.1.1}$$

Where p is pressure, p_s and p_t is the surface and top pressure respectively in the model.

The model physics include the radiative transfer package and planetary boundary layer schemes, convective and non-convective precipitation schemes, the land surface and ocean flux schemes, and atmospheric aerosol. The radiative transfer scheme employs the National Center for Atmospheric Research Community Climate Model (CCM3) radiation package which includes greenhouse gases (H2O, CO2, O3, CH4, N2O, and CFCs), solar radiation, cloud water and ice effect, and atmospheric aerosols (Kiehl at al. 1996, see details in CCM3 document). For solar radiative transfer calculations, delta (δ) - Eddington approximation (Briegleb, 1992) is used to account for large forward scattering by clouds and aerosols. In this scheme, the cloud influence on solar radiation is determined by three cloud parameters: fractional cover, water content and effective radius of cloud droplets. The aerosol direct effect is parameterized with three quantities: extinction optical depth (τ), single scattering albedo (ω) and asymmetry parameter (g), all are functions of wavelength. Interactions of aerosol with thermal infrared radiation are not included in the model. Such simplification would not introduce significant uncertainty for our study because smoke aerosol optical depth decreases rapidly with increasing wavelength.

The formation of precipitation in RegCM3 is represented as two forms: resolvable scale (large scale) precipitation and convective (subgrid) precipitation. The resolvable scale precipitation are represented via the subgrid explicit moisture (SUBEX) scheme

described by Pal et al. (2000), which accounts for the subgrid-scale variability of cloud water and includes formulations for the autoconversion of cloud water into rain water, the accretion of cloud droplets by falling raindrops, and the evaporation of falling raindrops. The cloud fractional cover is computed from relative humidity, and clouds form when the relative humidity exceed a certain threshold below grid cell saturation. The moist convection and precipitation are parameterized by the Grell (1993) cumulus scheme, which is a one-cloud version of Arakawa-Schubert (1974) scheme with the inclusion of downdraft when activated. The scheme is triggered when a low-level parcel is lifted less than 50mb before reaching the level of free convection and the cloud depth exceeds 150mb. The subgrid precipitation is a function of the amount of condensation in the updraft, the cloud-base mass flux, and precipitation efficiency function calculated from the mean wind shear in the lower troposphere. Grell scheme is chosen because it could success in simulating the patterns of precipitation over tropical South America, although it underestimated the magnitudes of both precipitation and temperature (Rauscher et al. 2006; Fernandes et al. 2006; Seth et al. 2006).

Over the ocean, the sea surface temperature (SST) dataset is prescribed with monthly averages of measurements, and ocean surface fluxes are calculated using a scheme by Zeng et al. (1998), which describes all stability conditions and includes a gustiness velocity to account for the additional flux induced by boundary layer scale variability. Over the land, the Biosphere-Atmosphere Transfer Scheme (BATS 1E) (Dickinson et al, 1993) is employed to compute surface net solar radiation, sensible and latent heat fluxes, momentum fluxes and surface temperature based on the vegetation and soil types.

Boundary layer physics is formulated following the non-local scheme of Holtslag et al. (1990) which considered the dry deep convection induced nonlocal turbulent transport, but dry convective adjustment is not used.

RegCM3 also requires initial conditions and time-dependent lateral boundary condition for the wind components, temperature, surface pressure, and water vapor.

3.2 Simulation Design

The choice of model domain in a regional climate model simulation can influence model sensitivity to various internal and external forcings (*Seth and Giorgi*, 1998). This study includes tropical and subtropical South America and the surrounding oceans (80^o W ~ 20^o W, 35^o S ~ 5^o N) as illustrated in Fig. 3.2.1 for the simulation domain. The area of this domain is about 5400×5400 km^2, which is large enough to avoid the influence of domain boundary on simulated atmospheric fields inside of the Amazon basin. Its atmosphere has 18 levels, with 7 levels in the lowest 1.5 km of atmosphere, and a horizontal resolution of 60 km.

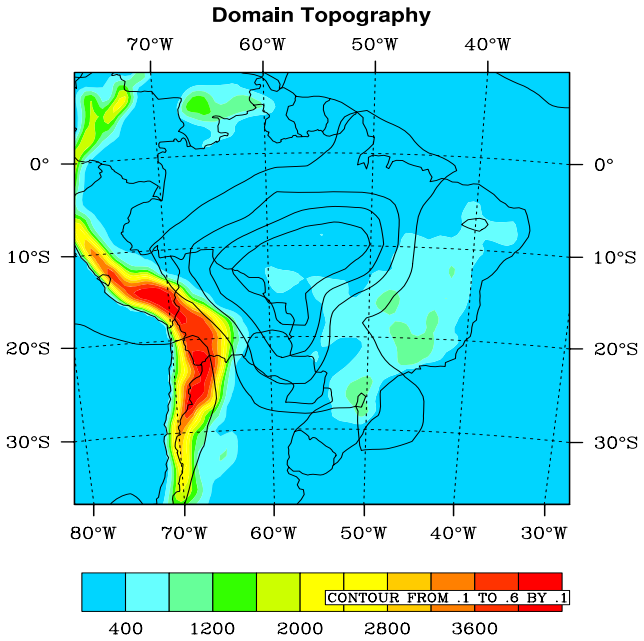

Figure 3.2.1. RegCM3 domain and topography (m). Unfilled contour represents aerosol optical depth at 550 nm in 2001. The contour interval is 0.1 from 0.1 to 0.6

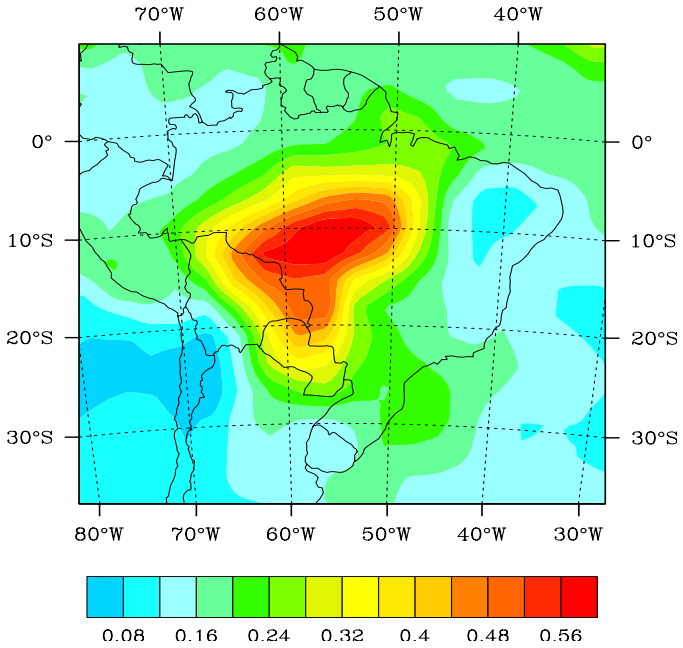

Figure 3.2.2. Distribution of aerosol optical depth at 550 nm for September in 2001 derived from an integration of MODIS retrievals and GOCART simulations.

For this study, we choose the period of August to October 2002 as the peak season for burning in South America. Satellite observation of clouds and aerosols from the Moderate Resolution Imaging Spectroradiometer (MODIS) on the EOS-Terra satellite showed a clear signal of reduced warm cloud fraction with increasing AOD over the Amazon in 2002, implying a dominance of "cloud burning" as expected from the aerosol semi-direct effect (*Koren et al.*, 2004; *Yu et al.*, 2007). This study used monthly averaged aerosol fields from a combination of the MODIS retrievals and the Goddard Chemistry Aerosol Radiation and Transport (GOCART) model simulations to achieve an optimal geographical distribution of AOD (*Yu et al.*, 2003). Figure 3.2.2 shows distributions of AOD at 550 nm for September. The spatial distributions of the SSA and asymmetry parameter (g) are obtained from GOCART simulations (*Chin et al.*, 2002). Averaged over the smoke region, the aerosol SSA is about 0.86 and g is about 0.7. These values do not have large spatial variation in the region of our study. This value of SSA is much smaller than that obtained from AERONET retrievals (*Dubovik et al.,* 2002) but is within the large range of in situ measurements for aged regional smoke as summarized in Reid et al. (2005). The MODIS-GOCART integrations are only available for 2001, and their aerosol forcing could be somewhat weaker than the smoke aerosol forcing during August-October of 2002 (*Procopio et al.*, 2004; *Yu et al.*, 2007). However, the use of the GOCART aerosol radiative forcing for our simulations should not change the processes through which aerosol radiative effect influences regional surface energy and water fluxes and circulation.

The aerosol effects over the Amazon region are examined with two sets of ten-member ensemble experiments. Ten ensemble simulations reduce the random error of the

surface solar flux over the smoke area where AOD ≥ 0.3 to 4 W m^{-2}, significantly less than the difference between the aerosol and control simulations (24 W m^{-2}). For each modeling experiment, RegCM3 is integrated from August to October when biomass burning is most active and the transition to monsoon takes place. August as a spin-up period is excluded from the analysis. Discussion of aerosol effects is focused on September when smoke aerosol has maximum loading.

The first set of the ensemble experiments is a control run without including aerosol, and is referred to as CONT hereinafter. These ensemble experiments were initiated with different dates varying from August 1-10, 2002, respectively. The second set of the ensemble experiments uses the same initial and boundary conditions as for the CONT experiment, but is forced by aerosol radiative effects, which in turn influence atmospheric and surface heating and clouds in RegCM3. This set of experiments is referred to as AERO hereinafter. A well mixed aerosol layer is placed from the surface to 3 km height in these simulations, as suggested by aircraft and satellite observations of the vertical range of smoke layer over the Amazon (*Andreae et al.*, 2004; *Landulfo et al.*, 2003; *Chand et al.*, 2006; *Yu et al.*, 2007; *Labonne et al.*, 2007). Table 2.2.1 summarized these two sets of experiments design.

Table 3.2.1 Summary of RegCM3 simulations.

	Aerosol	Aerosol mixing height	Time period
CONT with 10 samples	No	NA	Aug-Oct.
AERO with 10 samples	Yes	0~3 km	Aug-Oct.

The impact of aerosols radiative forcing is estimated as the difference between two

ensemble experiments (Δ ≡ AERO-CONT). Aerosol radiative forcing changes the lapse rate, water vapor, and cloud in our simulations. These changes together with the direct radiative effects of aerosol affect the surface fluxes and PBL structure.

3.3 Modification and Evaluation of the Model

Modification of land surface properties

Observations show that roots of the tropical forest in the Amazon could reach as deep as 14 to 18 m and are capable of transpiring considerable amounts of water throughout the dry season (*Nepstad et al.*, 1994). In the RegCM3 model, the default depth of soil and root layer for tropical forest is set to 3 m and 1.5 m, respectively. Such a shallow soil layer could not retain enough moisture to support realistic evapotranspiration (ET) in the Amazon. As a result of this problem, the model is known to substantially underestimate surface latent heat flux during the transition season (*Gash and Nobre*, 1997). Similar to that done by *Kleidon and Heimann* (2000), we used deeper rooting depths for a tropical forest to mitigate this problem. The depth of soil and root layer for a tropical forest was increased to 4.5 m and 3 m, respectively. We also changed the ratio of root distribution between the upper soil layer (0.1 m) and root zone soil layer (3 m) from 0.8 to 0.4, such that more roots are allocated in the root zone soil layer. These modifications have increased the availability of water for root uptake and improved the daily mean surface fluxes. Table 2.3.1 compares the monthly mean sensible heat flux (SH), latent heat flux (LH), surface net solar radiation (SR), Bowen ratio (BR=SH/LH), and surface temperature (T) obtained from three sets of RegCM3 simulations and those from flux tower observations during September 2002 at two tropical forest sites in Brazil,

namely Tapajos (3.01°S, 54.58°W, denoted as K83) and Ji Parana (10.07°S, 62.93°W, denoted as RJA) (*von Randow et al.*, 2004; *da Rocha et al.*, 2004; *Goulden et al.*, 2004). The simulated surface solar fluxes agree with observations within 10-20%. However, the original RegCM3 land scheme overestimates the sensible heat flux and underestimates the latent heat flux substantially, leading to a Bowen ratio of 3.8, an order of magnitude larger than the observed value of 0.33. The use of deeper root depths increases the ET and reduces the sensible heat flux, yielding a Bowen ratio that is in good agreement with measurements. Inclusion of the aerosol radiative forcing brings the Bowen ratio yet closer to the observations.

The formation of shallow clouds and deep convection strongly depend on the depth and static stability of the daytime PBL (*Williams and Renno*, 1993; *Fu et al.*, 1999; *Betts and Jakob*, 2002). The latter is controlled by diurnal changes of the surface fluxes. Figure 3.3.1 shows the diurnal cycle of SH and LH for September from RegCM3 simulation and tower observations. Clearly, RegCM3 with the modified root depth and vertical distribution still overestimates SH and underestimates LH during the daytime, especially at noon when the solar radiation is at its maximum. Thus simply increasing root zone depth and its fraction in deeper soil of the model cannot alone provide sufficient soil moisture to support a realistic daily maximum LH. Observations over the Amazon forest near Manaus in September 1995 showed that the soil moisture content in the upper 4 m of soil was about 1900 mm (*Malhi et al.*, 2002), whereas averaged total forest soil water content in the 3 m layer of RegCM3 is only about 1000 mm. Given our focus on obtaining realistic surface fluxes rather than on improving the physics of the land surface process, we fixed the soil moisture in the root layer to be 80% of the field capacity over

the tropical forest area. This modification fixes soil water in the forest root zone at approximately 1.4 m, consequently enabling RegCM3 to obtain a more realistic daily mean of the land surface fluxes and an improved diurnal cycle of these fluxes over the Amazon during the transition season (Fig. 3.3.1).

Table 3.3.1. Comparison of monthly mean sensible heat (SH, units: W m^{-2}), latent heat (LH, unit: W m^{-2}), Bowen ratio (BR=SH/LH), surface net solar radiation (SR, units: W m^{-2}), and 2 m air temperature (T, units: K) between RegCM3 simulations and measurements by flux tower for September 2002.

Sites	Variables	RegCM3 simulations			Flux Tower Observations
		Original Land Scheme	Modified-Roots Land Scheme	Modified roots Land Scheme with Aerosols	
Tapajos (3.01S, 54.58W)	SH	110	42	40	33
	LH	29	120	113	101
	BR	3.8	0.35	0.35	0.33
	SR	216	212	180	225
	T	304.7	300.6	299.8	300.3
Ji Parana (10.07S, 62.93W)	SH	83	42	27	28
	LH	54	104	101	99
	BR	1.5	0.40	0.27	0.28
	SR	198	202	200	220
	T	306.8	300.7	300.0	299.0

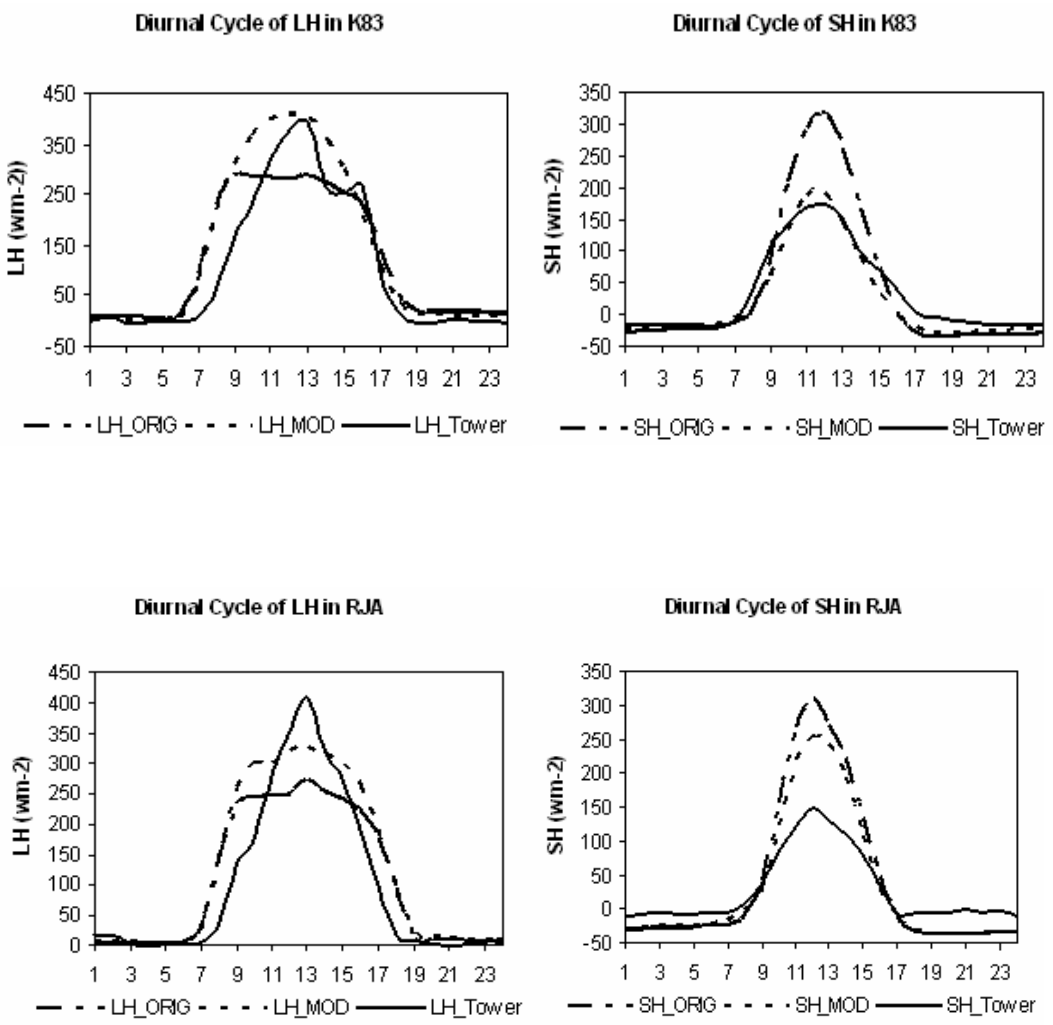

Figure 3.3.1. Diurnal cycle of LH and SH simulated by RegCM3 compared with in situ observations. ORIG represents theFigure 1using original RegCM3; MOD represents the simulation with modified soil moisture treatment as described in Section 3.1; Tower represents observations by flux tower. Unit :W m^{-2}.

3.4 Evaluation of the RegCM3

Figure 3.3.2 shows the 850 hPa wind field from the ECMWF short-term forecast product and RegCM3 CONTS simulations. The simulated pattern of wind in the RegCM3 is similar to that of ECMWF, but its simulated wind speed is weaker over southern Amazonia. The spatial pattern of change of geopotential height at 500 hPa from September to October, a main indicator of the transition from dry season to the monsoon onset, is well simulated in the RegCM3 (Fig. 3.3.3).

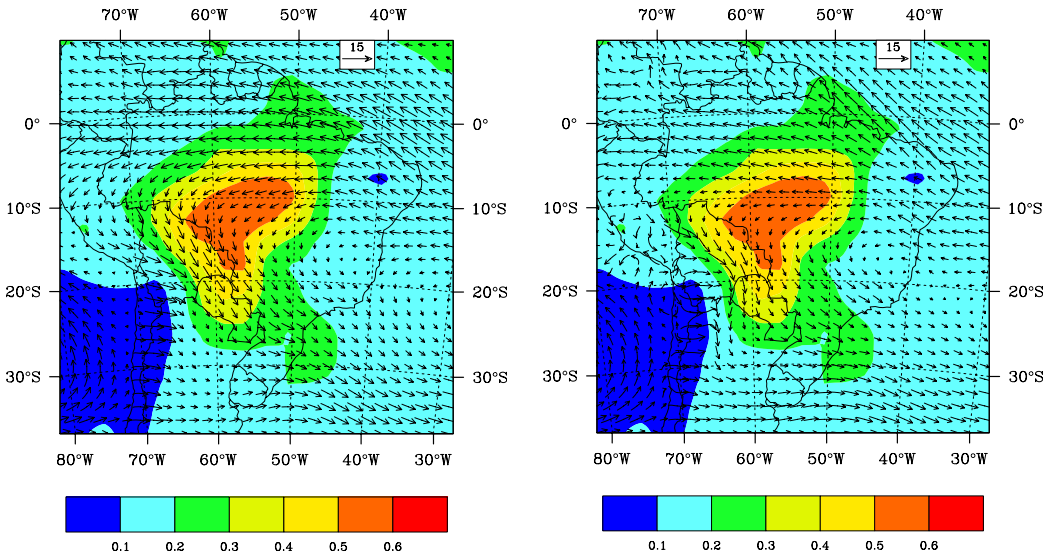

Figure 3.3.2. Monthly mean 850hPa wind field obtained from NCEP and RegCM3 for September 2002. The filled contour is aerosol optical depth in Sep. 2001.

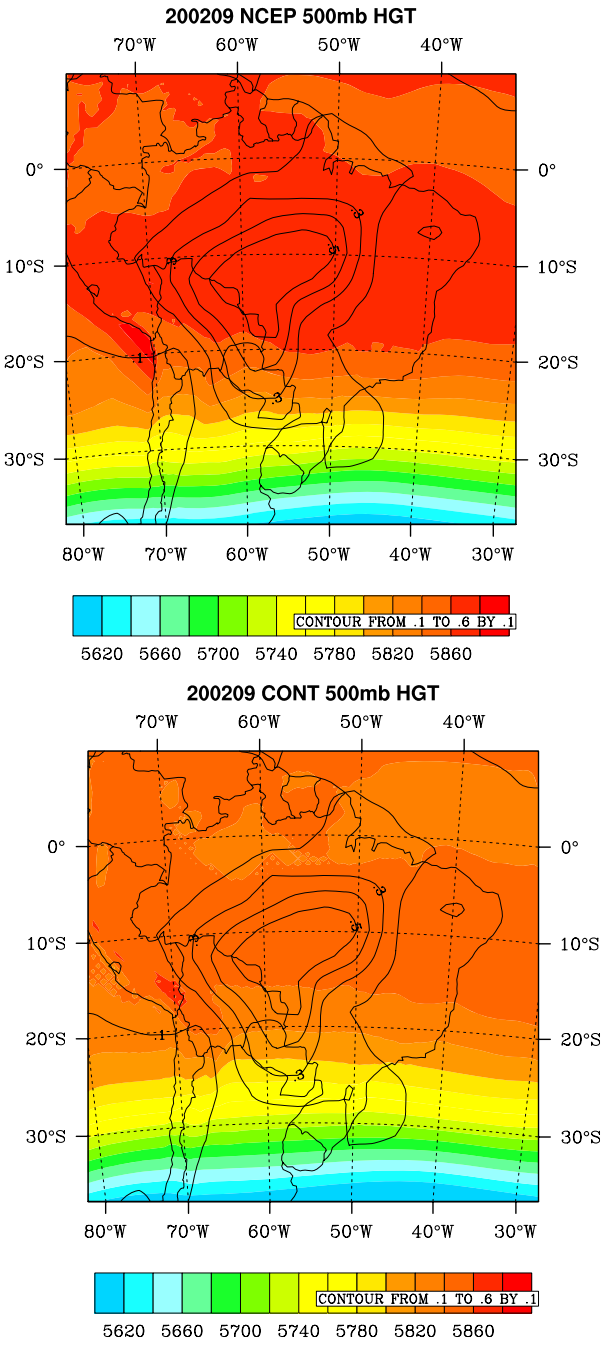

Figure 3.3.3. Monthly averaged 500hPa geopotential height derived from NCEP and RegCM3 for September 2002.

CHAPTER 4[1]

AEROSOL IMPACT ON THE ATMOSPHERE-LAND INTERACTION

This Chapter evaluates the smoke aerosol direct and semi-direct effects by comparing the results of the ensemble AERO and CONT simulations. Unless stated otherwise, all variables in the analysis are averaged over September at the peak of biomass burning.

4.1 Radiation and Surface Fluxes

The aerosol radiative forcing calculated at the top of atmosphere (ΔF_{TOA}, positive value for downward radiative flux) for clear-sky and whole-sky conditions are shown in Figs. 4.1.1a and 4.1.1b, respectively. Smoke aerosols reflect solar radiation back to the space resulting in a negative ΔF_{TOA}. They also absorb solar radiation. Such aerosol absorption of solar radiation reduces the planetary albedo and contributes to a positive ΔF_{TOA}. Thus the influences on ΔF_{TOA} from scattering and from absorption by smoke aerosols oppose each other. For a darker land surface and for clear-sky, the reflection is larger, and consequently $\Delta F_{TOA,clear}$ is negative with a spatial distribution that is similar to that of the AOD distribution and peaking at approximately -8 W m^{-2} over the maximum

[1] This chapter is for "A regional climate model study of how biomass burning aerosol impacts land-atmosphere interactions over the Amazon" published at *J. Geophys. Res.* 2008 (113, D14S15, doi: 10.1029/2007JD009449.) Authors are: Y Zhang, R. Fu, H. Yu, R. E. Dickinson, R. N. Juarez, M. Chin, and H. Wang

AOD region (Fig. 4.1.1a). For a bright surface, i.e., where there is snow cover over the Andes Mountains, the planetary albedo is reduced by the smoke aerosols and the forcing is positive.

The whole-sky radiative forcing ($\Delta F_{TOA,total}$) is affected by both aerosol scattering and absorption and change of cloud properties, i.e., fractional cover and cloud liquid water path. Therefore its pattern (Fig. 4.1.1b) does not necessarily match that of the AOD distribution. Indeed, the peak magnitudes of $\Delta F_{TOA,total}$ (~±22 W m^{-2} relative to 8 W m^{-2} uncertainty due to random errors of the ensemble simulations) are several times as large as the clear sky negative value indicating dominance by the cloud property changes. The role of cloud contributions to $\Delta F_{TOA,total}$ is isolated in Fig. 4.1.1c by subtracting it from $\Delta F_{TOA,clear}$ showing it to be positive (i.e., a decrease of cloud fraction or cloud liquid water) over most of the Amazonian region but negative (increases cloudiness) over northwestern Amazonia.

Figure 4.1.2 shows change of the solar radiative forcing by aerosols at the surface ($\Delta F_{Surface}$) for clear-sky and whole-sky, positive for a reduction of cloud fraction or liquid water path. Both the scattering and absorption of the smoke aerosols decrease the amount of solar energy at the surface by as much as 40 W m^{-2} (or 15%) for clear-sky conditions over the central Amazon. The spatial pattern of $\Delta F_{Surface,clear}$ generally follows that of AOD. For whole-sky conditions, the spatial pattern differs as reduction of SR ($\Delta F_{Surface,total}$) by smoke aerosols and is compensated by the reduction in cloud fraction that allows more solar radiation to reach the surface and thereby weakens aerosol direct radiative effect, mostly over the smoke areas (30 W m^{-2}) where AOD > 0.3. The whole-

sky surface solar radiation reduction over the smoke area is about 10 W m^{-2} less than the clear-sky reduction.

The forcing efficiency, defined by the aerosol forcing in clear-sky normalized by the AOD, is about -10 ~ -15 W m^{-2}/AOD for clear-sky at the TOA and -70 ~ -80 W m^{-2}/AOD at the surface (as shown in figure 4.1.3). The TOA values are in the lower end of the published range but the surface values are consistent with AERONET and other measurements (*Yu et al.*, 2006; *Zhou et al.*, 2005, *Procopio et al.*, 2004).

The change of solar heating changes atmospheric stability and surface heat fluxes. Figure 4.1.4 shows the consequent perturbations of surface fluxes of sensible heat (SH) and latent heat (LH). A reduction of SH of up to 25 W m^{-2} occurs primarily over the smoke area (AOD>0.3). That largely balances the reduction of net solar flux. The reduction of LH is weaker, in part because of an increase of vegetation transpiration near local noon, and has no obvious pattern.

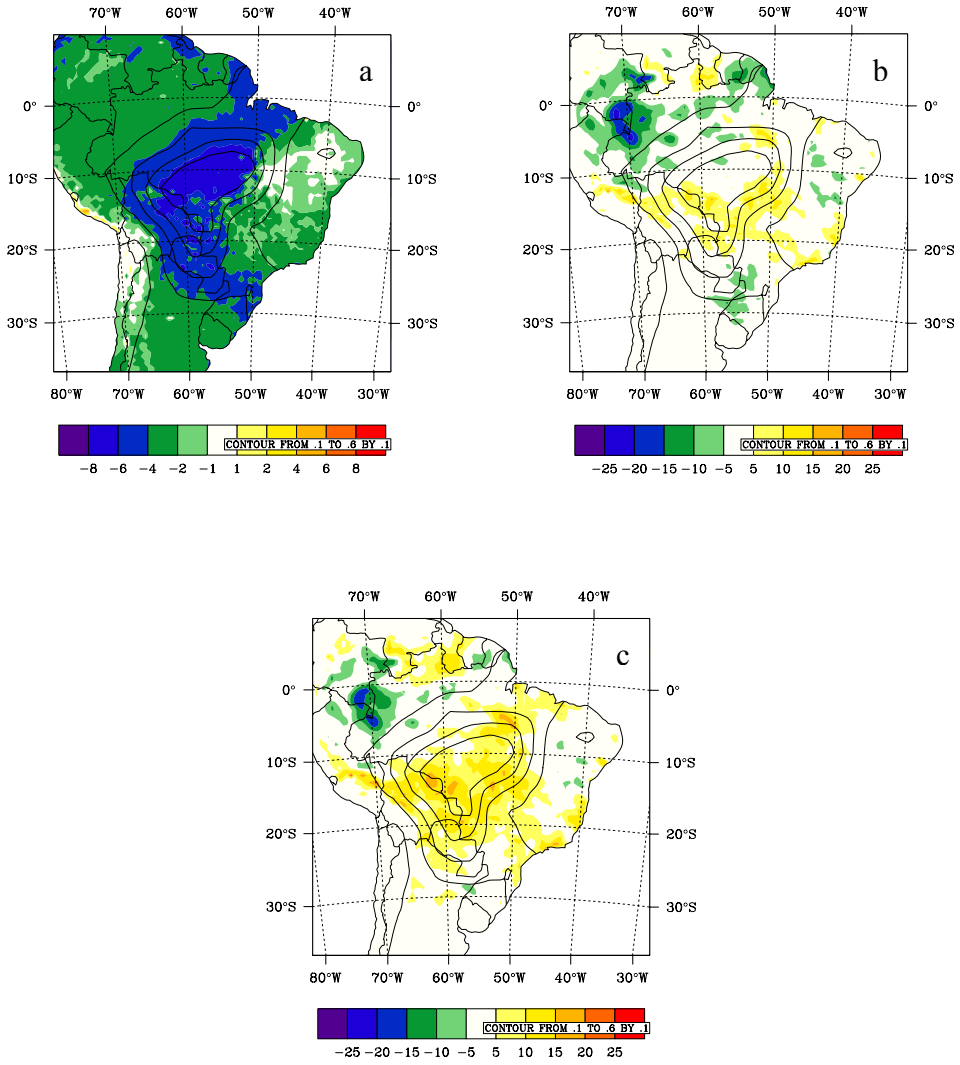

Figure 4.1.1. Difference in monthly daily mean TOA net downward solar radiation (W m^{-2}) between AERO and CONT for a) clear-sky condition, b) whole-sky condition and c) the TOA forcing by changes in cloud properties.

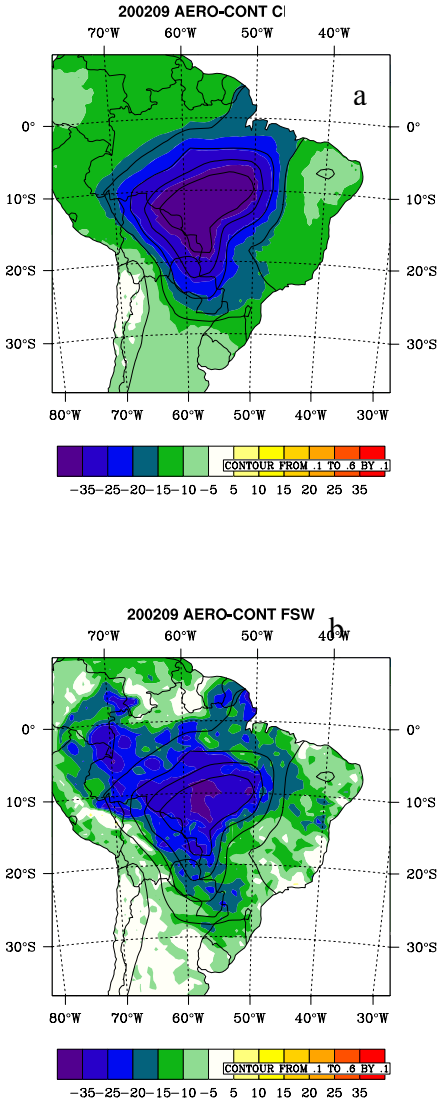

Figure 4.1.2. Difference of monthly average solar flux (W m^{-2}) at surface between AERO and CONT for a) clear-sky condition and b) whole-sky condition.

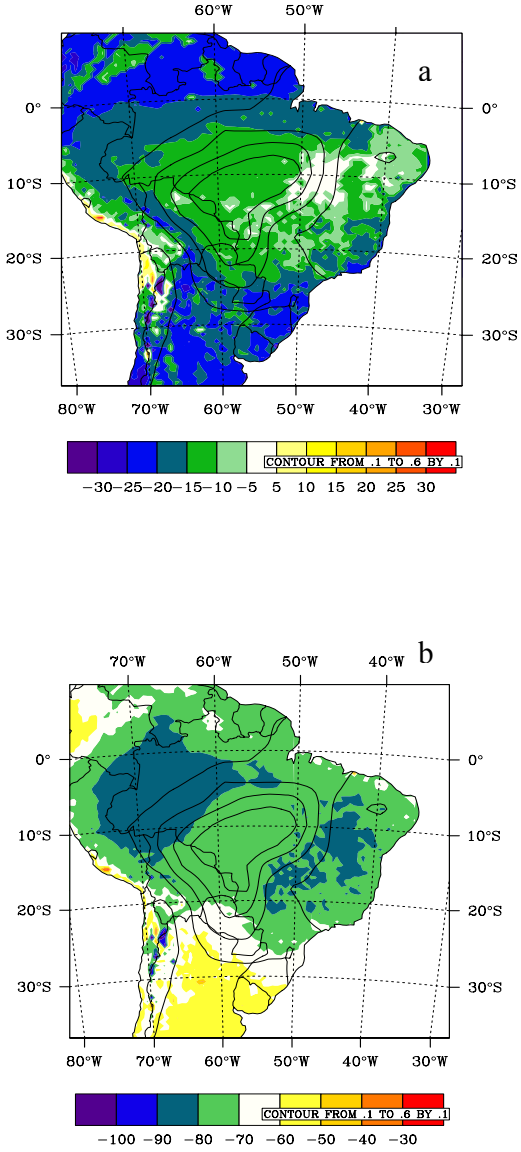

Figure 4.1.3. The forcing efficiency (forcing/AOD) of aerosol for a) TOA and b) Surface.

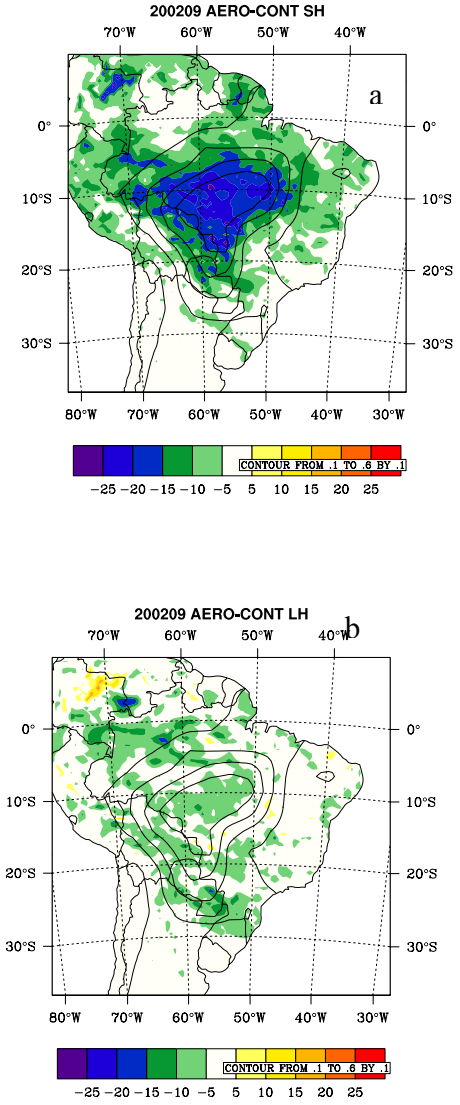

Figure 4.1.4. Difference of (a) monthly sensible heat flux (SH, Wm^{-2}); and (b) monthly latent heat flux (LH Wm^{-2}) between AERO and CONT simulations.

4.2 Planetary Boundary Layer Evolution

The influence of smoke aerosols on the diurnal cycle of the surface fluxes and on the PBL are examined by area mean changes of these variables over the smoke center, i.e., where AOD > 0.3.

Figure 4.2.1 shows the diurnal variation of the clear-sky and whole-sky surface solar fluxes (SR), respectively, in the CONT experiment as well as the changes due to the radiative effect of smoke aerosols. Without smoke aerosols, SR reaches a maximum at noon for both cases. The total cloud forcing, i.e., the difference between whole-sky and clear-sky SR, is as much as -200 W m^{-2} in the afternoon. With aerosols, SR at the surface for clear-sky is reduced by about 80 W m^{-2} from 8 LST to 15 LST. For whole-sky, this aerosol forcing is weakened due to cloud reduction between 13 LST and 17 LST.

Figure 4.2.2 shows the aerosol induced changes of SR and net outgoing infrared radiation (LW), as well as those of SH and LH. In general, reduction of SR is mostly balanced by reduction of SH, and only secondarily, by changes of LH and LW. SH decreases significantly during the day with its largest reduction of about 70 W m^{-2} (25%) at 11 LST. Daily average changes of SH and LH in the selected domain are -15 W m^{-2} and -5 W m^{-2}, respectively. The LH change is about 1/3 of the SH change, so the Bowen ratio is lowered by 0.14 (about 30%). The model determines SH over vegetation by the difference of air temperature between that within and that above the foliage. The reduction of SH is related to a greater reduction of leaf surface temperature than the reduction of air temperature above. As shown in Fig 4.2.3, the leaf surface temperature is reduced by the aerosol cooling effect by as much as 1.7°C at 11 LST, whereas the air temperature reduction at 2 m above the foliage is only 1.3°C.

Why does LH decrease in early morning and late afternoon, but increase from late morning to early afternoon (Fig. 4.2.2)? Figure 4.2.4 shows that the evaporation from canopy interception increases uniformly, presumably because of the increase in precipitation. This term is more than compensated by a decrease in transpiration in the early morning and late afternoon. But during late morning to early afternoon, transpiration increases slightly in the presence of aerosols, leading to a small increase in LH. The cooler midday temperature in the presence of aerosols reduces the midday vapor-pressure term and so decreases the stomatal resistance, hence increases the transpiration (*Steiner, et al*., 2005).

Diurnal changes in the height of the PBL are determined by the surface buoyancy flux and capping inversion. Smoke aerosols reduce the surface SH and convectively driven turbulence, and also warm the lower troposphere. These effects can strengthen the capping inversion and decrease the height of the daytime PBL (*Yu et al.*, 2002). Previous field measurements in the Southern Amazon suggest that the daily maximum height for PBL varies from 250 m to 1.25 km over forests and from 110 m to 2.22 km over pasture during dry season (*Nobre et al*., 1996). Fig. 4.2.5 shows that the PBL in our simulations varies from 400 m to 2 km. The simulated daily maximum PBL height is about 500 m higher than that observed over forest. This discrepancy is in part caused by an overestimate of daily maximum surface sensible flux, and presumably also by a weakness in the treatment of PBL physics. Given the model's tendency to overestimate surface sensible flux, the change of PBL due to smoke aerosols radiative forcing may also be overestimated. The smoke aerosols delay the growth of the PBL in the morning and reduce its daytime height. The maximum reduction of the PBL height is about 300 m

(16%) and occurs at 11 LST, much larger than the 40 m uncertainty due to random errors of ensemble simulations. The change of the PBL height in the late afternoon is not as strong as in the morning, consistent with the weaker reduction of the SH due to 'cloud burning'. The weaker influence of aerosols on the PBL height in early afternoon is consistent with the weaker reductions of SR and SH (Fig. 4.2.2).

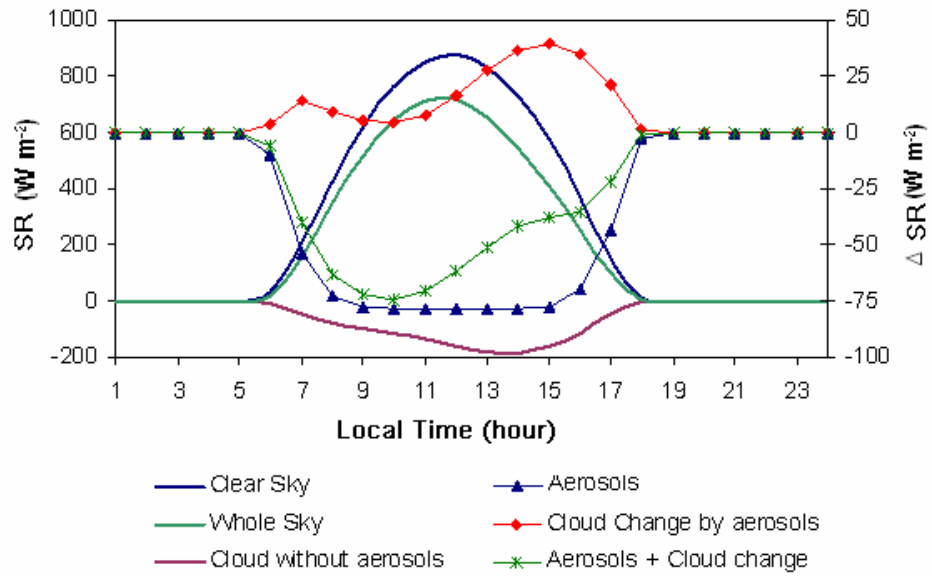

Figure 4.2.1. Diurnal cycle of surface net solar flux SR (left axis) and its change induced by smoke aerosols, aerosol induced cloud changes, and smoke aerosols plus cloud changes (right axis) averaged over area where ADO > 0.3 in September. Units:W m^{-2}.

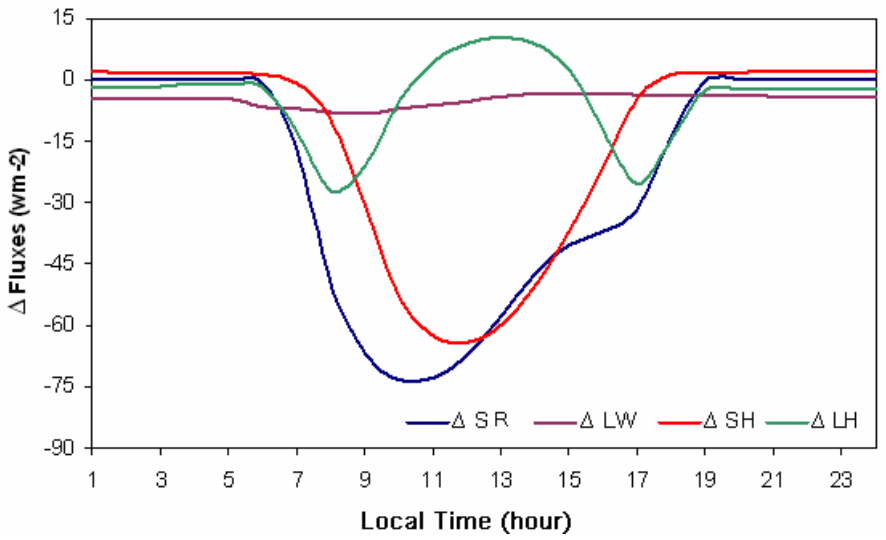

Figure 4.2.2. Diurnal cycle of changes of surface net solar radiation (ΔSR), outgoing infrared radiation (ΔLW), sensible heat flux (ΔSH), and latent heat flux (ΔLH) averaged over area where ADO > 0.3 in September. Units:W m^{-2}.

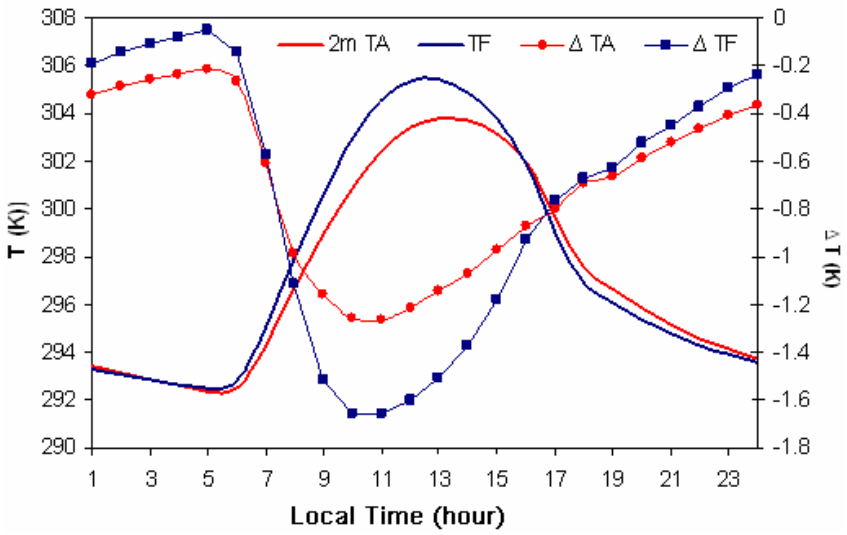

Figure 4.2.3. Diurnal cycle of foliage surface temperature (TF) and air temperature (TA) at 2 m (left axis, solid curves) and their changes due to aerosols (right axis, solid curves with symbols) averaged over area where ADO > 0.3 in September.

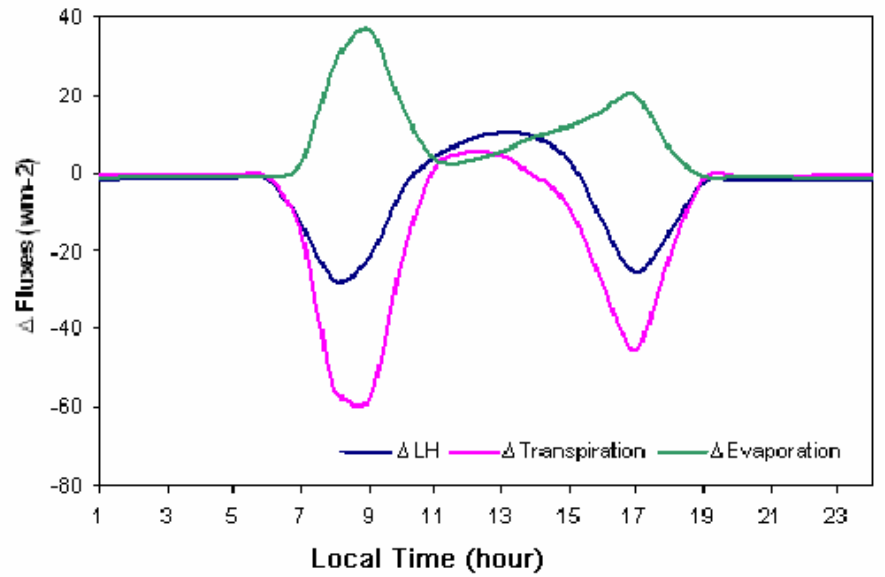

Figure 4.2.4. Diurnal cycle of the change in surface latent heat flux (ΔLH), and its transpiration (ΔTranspiration) and evaporation (ΔEvaporation) component between the AERO-CONT simulations averaged over area where ADO > 0.3 in September.

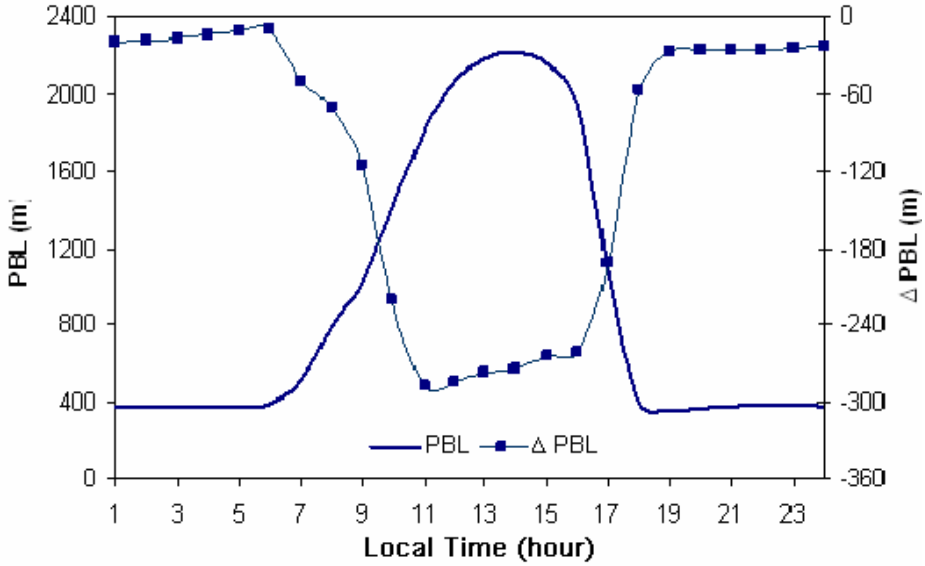

Figure 4.2.5. Diurnal evolution of the planetary boundary layer (PBL) height (left axis, solid curve) and its change due to aerosols (right axis, solid curve with symbol) averaged over area where AOD > 0.3 in September.

4.3 Effect on Clouds

Smoke aerosols can affect atmospheric thermodynamics by absorbing solar radiation and consequently can influence the cloud fraction through the following processes: a) by decreasing surface sensible heat flux and increasing atmospheric stability and thus reducing turbulence; b) by changing the relative humidity (RH) either due to changing dry air entrainment at top of the PBL or due to changing temperature; c) by changing horizontal pressure gradient and regional circulation.

Figure 4.3.1a shows the spatial distribution of the difference (AERO-CONT) in cloud liquid water path (LWP) integrated between the surface and 2 km and the difference of the wind at 1.5 km within the daytime PBL. No obvious change in the cloud LWP within the daytime PBL appears in the smoke areas. However, in equatorial Amazonia to the north and northwest of the smoke area, cloud LWP increases by as much as 20 g m^{-2} or 40% to 50%. Figure 4.3.1b shows the changes of cloud LWP for the layer from 2 km to 3 km and the change of wind at 3 km for the AERO-CONT. A large-scale decrease of cloud LWP between 2 and 3 km layer can be seen both inside and to the north of the smoke areas. However over equatorial Amazonia to the north of the smoke area, the increase of cloud LWP below 2 km more than compensates for the reduction of cloud LWP above 2 km, leading to a net increase of cloud LWP in that region. Within the smoke area, the vertically integrated LWP decreases as a result of direct and semi-direct effect of smoke aerosols. In October (figure 4.3.2), the pattern of cloud LWP change is similar to that in September. Cloud LWP between the surface and 2 km increases by as much as about 23 g m^{-2} to the northwest of the smoke area, and cloud LWP between 2 and 3 km decreases (by about 10 g m^{-2}) in the smoke area.

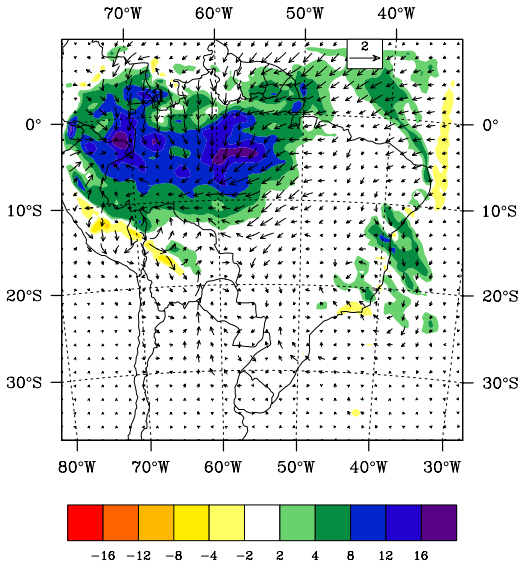

b

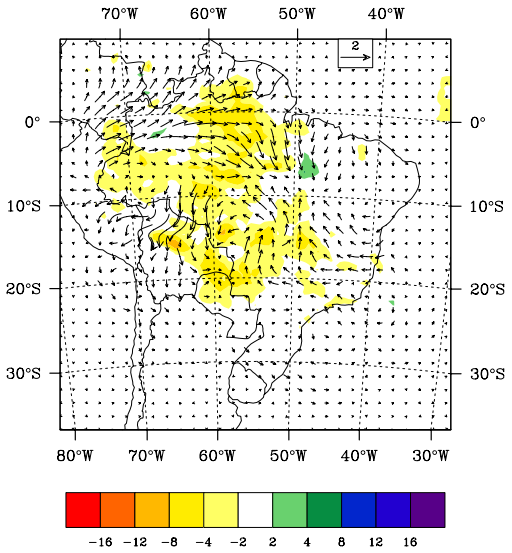

Figure 4.3.1. Aerosol induced a) change in cloud LWP (g m^{-2}) integrated between surface to 2 km and the change of circulation which is indicated by the change of the wind at 1.5 km (b) changes in cloud LWP between 2 km to 3 km and change of the wind at 3km in the September.

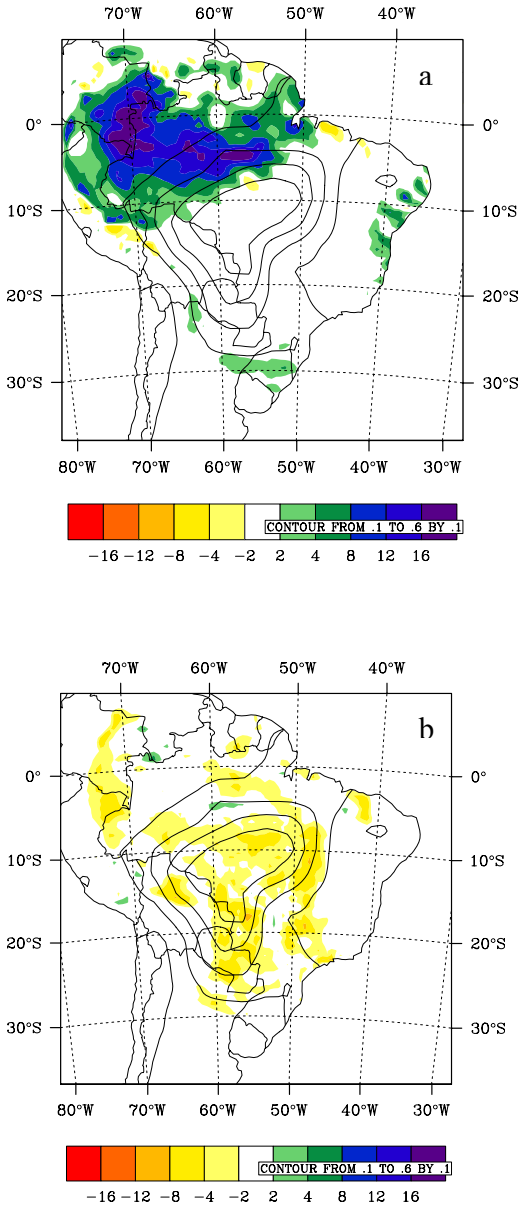

Figure 4.3.2. Aerosol induced a) change in cloud LWP (g m^{-2}) integrated between surface to 2 km (b) changes in cloud LWP between 2 km to 3 km in the October.

What might cause the changes of LWP shown in Figure 4.3.1? Aerosols are prescribed to be vertically uniform within the smoke area. However, the solar radiation absorbed by smoke aerosols is strongest at the top of the smoke layer. This aerosol absorption increases the air temperature, hence reducing the lapse rate and enhancing the capping inversion. Weaker turbulence also reduces the height of the daytime PBL. Both processes decrease clouds in the 2 km to 3 km layer right above the top of the PBL.

What could cause the large-scale increase of cloud LWP in the PBL over equatorial Amazonia outside of the smoke area? Figure 4.3.1 shows atmospheric circulation perturbations at different levels. This alteration of the regional circulation results from surface cooling in the smoke area that leads to an anomalous lower-level moisture divergence in the smoke area and moisture convergence and higher humidity in the upwind direction of the smoke area in equatorial Amazonia. High humidity in turn increases LWP in the PBL over the equatorial Amazon.

4.4. Discussion

A sensitivity test assuming an aerosol diurnal variation in RegCM3 was conducted to examine how such a diurnal variation of the aerosol would influence our results. The diurnal variation of AOD is taken from observation of tropical biomass burning smoke as described in *Smirnov et al*. (2002, Figure 2), which shows a 10% lower AOD at 10 am LST (the daytime minimum AOD) and 20% higher AOD at 4pm LST (the daytime maximum AOD) compared to its daily mean. Our test shows that this diurnal change leads to aerosol radiative forcing at the surface 10% smaller in the morning and 10% higher in the afternoon compared to that obtained by using daily mean AOD. The

disproportional smaller increase of the aerosol radiative forcing at the surface in the afternoon is due to stronger reduction of clouds compared to that caused by daily mean AOD, which partially compensates the impact of daily maximum AOD on the surface solar flux. The changes in diurnal variation of SH and PBL relative to those forced by daily mean AOD are proportional to that of the surface solar flux. Since observation show that the AOD could exceed 2.0 for single days in September 2002, a sensitivity test with an AOD value of 2.0 in five random days was conducted. It gave a monthly reduction of surface incoming solar radiation of 34 W m^{-2} in the smoke area, and compared to the 30 W m^{-2} simulated using daily mean AOD.

We have also conducted a test using the GOCART aerosol radiative forcing and the initial and boundary conditions for the period of August-October 2001. This simulation showed similar patterns of changes in the surface fluxes induced by smoke aerosols as those obtained from using the initial and boundary conditions for August-October 2002. Evidently, the processes that control the aerosols radiative effect on surface fluxes, clouds, and the transition of monsoon circulation identified in this study are robust and do not change qualitatively with the specific years that might be chosen for simulations.

We have conducted a simulation over a larger domain (100^{o} W ~ 20^{o} W, 35^{o} S ~ 25^{o} N) to test the effect of the lateral boundary conditions on the northwest region. The aerosol induced increase of cloud LWP from 0 to 2 km over the northwest is 18 g m^{-2}, not significantly different from the 20 g m^{-2} obtained from our small domain simulation.

This study suggests somewhat different influences of the direct and semi-direct effects of aerosols on the PBL structure and surface fluxes than have been found in previous studies. In particular, atmospheric single column models without inclusion of

cloud processes have shown that strongly absorbing aerosols (SSA=0.8) would raise the daytime PBL height (*Yu et al.*, 2002). However, the daytime PBL height in this study decreases by about 10%. Decrease of cloudiness in early afternoon also partially compensates for the smoke aerosol effects, leading to a stronger influence of the smoke aerosols on the surface in later morning than in early afternoon. Aerosol absorption stabilizes the PBL. This stabilization could be disturbed by surface heating of the biomass fires, which may cause a net increase of the PBL height. Since fire has not been included in the model, our results may not be applicable in a region of active fire. In addition, the vertical distribution of absorbing aerosol in the convective PBL is important for determination of cloudiness reduction (*Feingold et al.*, 2005) and can modify the PBL height. Thus our results might change if the vertical structure of the aerosol layer were very different from that assumed in our simulations.

By prescribing a uniform smoke aerosol forcing over most of the Amazon region (2° S ~ 22° S, 44° W ~ 70° W, excluding the Andes mountains), Liu (2005) have simulated a basin-wide reduction of cloud LWP over smoke area that he attributed to a weaker upward water transport from the PBL to the cloud layer and anomalous subsidence due to smoke. Our simulation uses observed spatial distribution of AOD and provides a more realistic Bowen ratio for the surface fluxes. Our results suggest a reduction of LWP in the smoke area, but an increase of LWP in the equatorial Amazon. The reduction of the LWP in the smoke area is due to a weakened southward moisture transport to this area and a shallower daytime PBL. The former would slow down the building up of lower troposphere moisture, thus convective available energy (CAPE), whereas the latter would reduce the probability for surface air to reach the level of free

convection. Both such changes could reduce the probability of atmospheric convection, a primary driver for transition from dry season to monsoon circulation. The reduction of the surface solar and sensible fluxes causes anomalous low-level moisture divergence in the southern Amazon in the smoke area and anomalous moisture convergence in equatorial Amazonia, leading to a dipole of LWP change and a weakening of the transition from dry to wet monsoon circulation.

4.5. Conclusions

We have applied the regional climate model RegCM3 to examine over Amazonia the smoke aerosol direct and semi-direct effect during a dry to wet transition season (August – October). By modifying the soil and plant root parameters and by adding soil water to mitigate the dry bias of soil moisture in the RegCM3, we are able to significantly reduce the discrepancies between the modeled diurnal cycle of the surface sensible and latent fluxes and those observed. The modeled changes occur both from the direct radiative effect of the aerosol and from changes in cloudiness. Changes are seen outside of the region of maximum aerosol as a dynamic response. A decrease of cloudiness in early afternoon partially compensates for the direct effects of smoke aerosols. Consequently, the strongest changes of surface flux and the PBL due to direct and semi-direct effects of the smoke aerosols occur in late morning. The reduction of net solar radiation in the smoke area at the surface (20 ~ 35 W m^{-2}) is mainly compensated by a reduction of surface sensible flux (15 ~ 25 W m^{-2}). Reduction of latent flux is only about 30% (5 ~ 15 W m^{-2}) of the sensible flux reduction. Inside the smoke area, cloudiness decreases with a maximum decrease occurring in the layer right above the daytime PBL

(2 km to 3 km above the surface). This decrease is presumably due to strong solar radiation absorption by smoke aerosols in this layer and to the reduction in the daytime PBL height and surface sensible fluxes. Outside of the smoke area in equatorial Amazonia, the cloud liquid water path increases with its maximum increase occurring below 2 km within the daytime PBL. An increase of lower-level moisture convergence in this region appears to be responsible for the increase of both specific and relative humidity in the PBL. Smoke aerosols, probably through their surface cooling, cause an increase of low-level moisture divergence in the smoke center and a compensating moisture convergence in equatorial Amazonia. Such a regional circulation change would delay the normal circulation transition from dry season to monsoon onset.

CHAPTER 5

AEROSOL EFFECTS ON RAINFALL OVER SOUTH AMERICA

5.1 Introduction

In Amazonia, biomass burning generated smoke aerosols dominate the atmospheric aerosol composition from June to October (Andreae et al., 1988; Artaxo et al., 1998). These smoke aerosols are mostly black and organic carbon. The black carbon strongly absorbs solar radiation and the organic carbon primarily scatters solar radiation (Penner et al. 1992, Hobbs et al. 1997). Such smoke aerosols reduce the surface solar flux, heat the local atmosphere, and thus modify the atmospheric thermodynamic structure. These changes, in turn, perturb regional circulation, cloud and the land-atmosphere interactions (*Zhang, et al.,* 2008, *Liu* 2005). However, whether and how such aerosol induced changes influence the development of monsoon circulation and rainfall in South America has remained unclear.

Many previous papers have investigated how smoke aerosols influence clouds, convection and the monsoon circulation of South America through field experiments, satellite observations and model simulations (e.g., *Andreae et al.,* 2004, *Kaufman et al.,* 2006, *Yu et al.,* 2002, *Liu* 2005). In particular, Liu (2005) first suggested that aerosols from biomass burning can weaken the South American monsoon circulation as inferred from a regional climate model with spatially uniform aerosol radiative forcing. Pathirana et al. (2007) found that heating by smoke aerosols stabilizes the atmosphere causing a reduction in rainfall. Zhang et al. (2008) used spatially varying aerosol forcing and a regional climate model with improved land surface energy partitioning to examine the

impact of smoke aerosols on the diurnal cycle of the atmospheric boundary layer and cloudiness over Amazonia. The present study differs from previous work by focusing on how aerosols influence the mechanisms that control the monsoon circulation transition. In doing so, it contributes to the understanding of the impact of aerosols on rainfall patterns. As in Zhang et al. (2008), the land surface partition into sensible and latent fluxes has been substantially improved in the regional climate model for Amazonian rainforest areas. Ensemble model simulations are used to ensure that the changes induced by aerosol radiative forcing are significantly greater than the random errors due to the internal variability of the model.

Biomass burning peaks from August to October annually with maximum concentrations in Southeastern Amazonia. This peak coincides with the monsoon transition from dry to wet season, characterized by rapid expansion of rainy area from northwestern to southern Amazonia (*Kousky* 1988; *Horel et al.* 1989; *Marengo et al.,* 2001). This monsoon circulation transition is initiated by an increase of surface radiation and resultant increases in latent and sensible fluxes, which lead to destabilization of the atmospheric thermodynamic structure and increase of moisture transport to Amazonia (*Li and Fu* 2004). In addition, cold front incursions from extratropical South America lift warm and humid surface air in Southern Amazonia and trigger the large-scale increase of rainfall and wet season onset (*Li and Fu,* 2006). This work explores whether or not smoke aerosols can influence these processes key to the monsoon circulation transition. In doing so, we aim to clarify the mechanisms through which smoke aerosols influence large-scale rainfall pattern.

Aerosols can influence rainfall in three main ways. Aerosols can act by scattering solar radiation and thus reduce the surface solar flux, and also by absorbing solar radiation and warming the aerosol layer. This is referred to as the aerosol direct effect. Aerosols can also change the lapse rate of the atmosphere and induce a dynamic response of the atmosphere flow. This is referred to as the semi-direct effect (*Hansen et al.,* 1997). The semi-direct effect can either increase or decrease rainfall locally and remotely (Koren et al. 2004; Kaufman and Koren 2006). Finally, aerosols can increase the number of small cloud droplets and thus albedo of the cloud (*Twomey,* 1977). This is referred to as the aerosol indirect effect. The indirect effect can either suppress light rain or invigorate heavy rain depending on the strength of the rainfall systems (Rosenfeld 1999; Andreae et al. 2004). In this study, we will examine the aerosol direct and semi-direct effects caused by the radiative forcing of aerosols.

5.2 Model Evaluation

Figure 5.2.1 compares the spatial distribution of rainfall for September obtained from the RegCM3 simulations, with that of the NOAA Climate Prediction Center data (CPC) at a resolution of $1^o \times 1^o$, and the National Aeronautics and Space Administration (NASA) Tropical Rainfall Measuring Mission data (TRMM) with a resolution of $0.5^o \times 0.5^o$, both also for September. The RegCM3 qualitatively captures strong rainfall centers over northwest and southeast Amazonia, as shown by both datasets. The magnitude of rainfall simulated by RegCM3 agrees closely with that of the CPC but is weaker than that shown by TRMM.

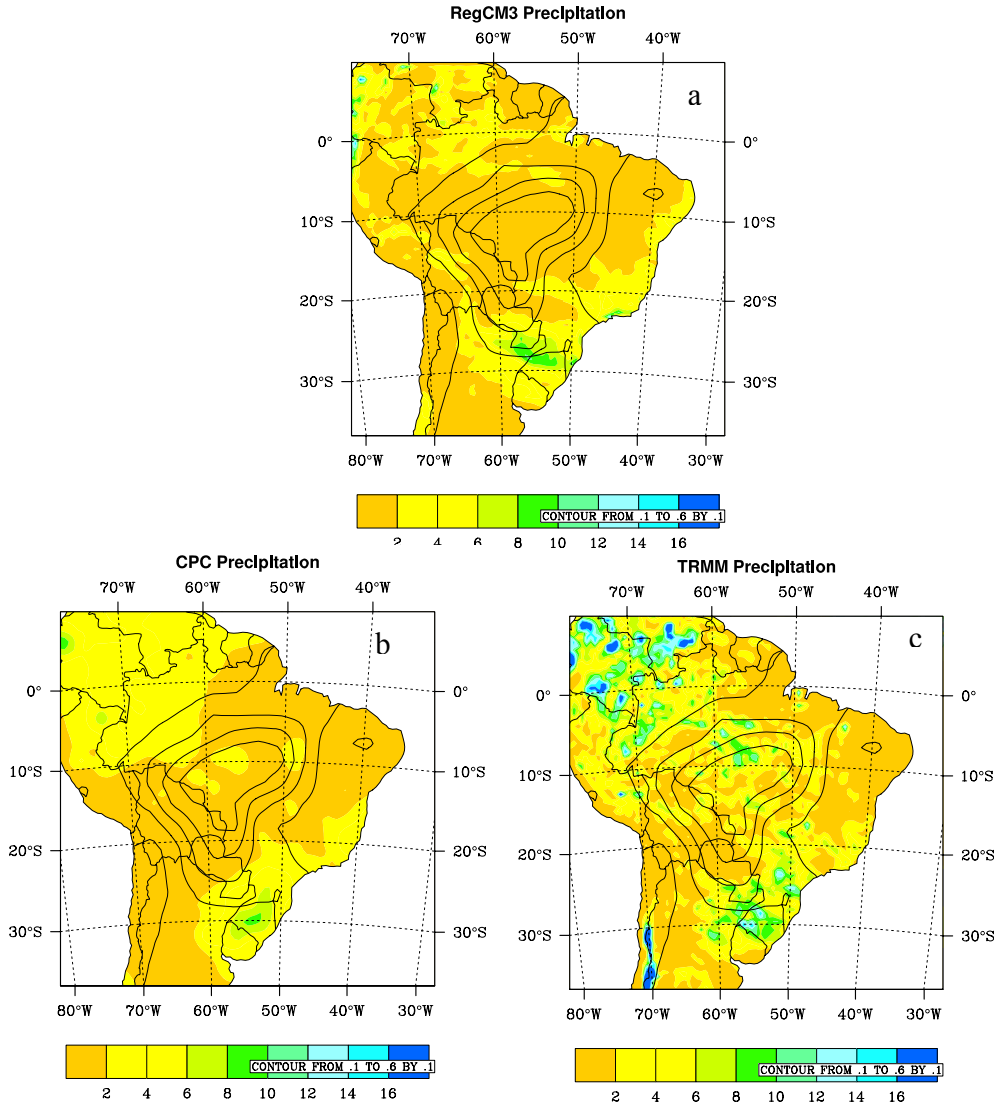

Figure 5.2.1. Ensemble monthly mean precipitation (unit: mm) derived from (a) RegCM3, (b) CPC, and (c) TRMM simulations for September 2002. The prescribed aerosol optical depth (AOD) is shown by contours with interval of 0.1.

5.3 Results

Our analysis mainly focuses on September at the peak of the smoke aerosol optical depth. Figure 5.2.1a shows that RegCM3 has only weak precipitation (1.0 mm day^{-1}) over the smoke area. Rainfall averages about 2.2 mm day^{-1} over Equatorial Amazonia. Previous ground-base and satellite observations showed that about a half of rainfall is generated by stratiform clouds in southern Amazonia (*Rickenbach, et al.,* 2002, *Petersen, et al.,* 2002). The non-convective rainfall and convective rainfall from our simulations is 1.4 and 0.8 mm day^{-1}, respectively, over equatorial Amazonia. Figure 5.3.1a shows the difference in rainfall between AERO and CONT in September, i.e., the influence of aerosols on rainfall. Rainfall in the smoke area changes very little (about 0.02 mm day^{-1} or 2%) despite heavy aerosol loading. However, the increase of rainfall is much more substantial (0.36 mm day^{-1} or 16%) over equatorial Amazonia where the smoke aerosol load is weak. The rainfall anomaly patterns induced by aerosols over northwestern Amazonia are consistent with the patterns of cloud liquid water and circulation anomalies at 850 hPa (Figure 4.3.1). Fig. 5.3.1a also shows a dipole pattern of rainfall change between southeastern Brazil and northeastern Argentina (20^o - 35^o S, 40^o - 65^o W). What processes could cause the aforementioned patterns of rainfall change? Fig. 5.3.1b shows changes of surface pressure and lower troposphere moisture divergence (925 hPa) induced by the aerosol radiative forcing to explore the cause of the rainfall change pattern within Amazonia. An increase of surface pressure occurs in the smoke center, as expected from a surface cooling and a more stable lapse rate due to the smoke aerosol influence. Without aerosols, the transition of the monsoon circulation, especially the moisture transport, is driven by a destabilization of the lower troposphere lapse rate and

surface pressure in southern Amazonia. The aerosol induced change works against these processes and weakens the surface pressure gradient, which drives the northerly wind. The strength of northerly wind dominates the moisture transport in Amazonia (*Wang and Fu* 2002, *Li and Fu* 2004). If this wind is diminished, moisture transport to southern Amazonia is reduced and the retention of moisture in northern Amazonia enhanced. These wind changes provide the dipole of moisture divergence change between the northwestern and southern Amazonia shown in Fig. 5.3.1b. These changes do not lead to significant rainfall decrease in southern Amazonia, because the meteorological conditions are too stable for rain in September even without aerosols (Fig. 1, Fu et al. 1999). However, the anomalous moisture convergence does significantly increase rainfall in northwestern Amazonia by the increasing moisture transported to that region in the lower troposphere.

The other dipole pattern of rainfall change in the southeastern subtropical South America (20^o - 35^o S, 40^o - 65^o W) also needs to be explained. Previous studies suggest that the incursion of extra tropical cold fronts and South American Low-level Jets (SALLJ) are important contributors to rainfall, especially during austral winter and spring (*Garreaud and Wallace* 1998; *Garreaud*, 1999, *Berbery et al.,* 2006). In previous studies, the cold fronts and associated baroclinic wave activities are well identified by a storm track index (e.g., *Xie and Arkin*, 1997, *Nakamura et al.,* 2002). For this purpose, we used a daily change of eddy meridional temperature flux at 700 hPa ($\delta\overline{v'T'}_{700hPa}$, *Hoskins and Valdes,* 1990). Fig. 5.3.2a shows the differences in $\delta\overline{v'T'}_{700hPa}$ and rainfall between the AERO and CONT ensemble simulations, i.e., the change of these fields induced by the smoke aerosol radiative forcing. A negative value of $\delta\overline{v'T'}_{700hPa}$

represents an increase in cyclonic activity in Southern Hemisphere. The pattern of RegCM3 simulated $\delta\overline{v'T'}_{700hPa}$ (not shown) is similar to the climatology of $\delta\overline{v'T'}_{700hPa}$ in Kodama and Tamaoki (2002, Fig.10b) for the period of 1979-1993. This agreement with observations suggests that the RegCM3 adequately captures the baroclinic wave activities in the region. The see-saw shape of $\delta\overline{v'T'}_{700hPa}$ change is similar to that of the pattern of rainfall change but with a 90˚ phase shift, namely the rainfall anomalies are maximum where the $\delta\overline{v'T'}_{700hPa}$ anomalies are near zero. Such a phase shift is expected because anomalous mid-tropospheric vertical motion, which causes rainfall anomalies, is driven by upper troposphere divergence or convergence induced by change in gradient wind. The gradient wind change is maximum in transition areas between anomalous cyclonic flow (trough) and anticyclonic flow (ridge) associated with the mid-latitude synoptic waves. The similarity of the patterns of the change of rainfall and $\delta\overline{v'T'}_{700hPa}$ (Fig. 5.3.2a) suggests that a shift of extratropical wave activity, presumably blocked by increasing stability in southern Amazonia, may cause the rainfall changes in the subtropical eastern South America. Fig. 5.3.2b shows the change of meridional winds in the troposphere along 20˚S across the South America. The northerly wind anomalous below 750 hPa between 40˚W and 60˚W, suggests an enhanced SALLJ and moisture export from southeastern Amazonia to southern Brazil, Paraguay and northern Argentina (*Berbery and Barros*, 2002). Thus, an enhanced northerly low troposphere wind and moisture export from Amazonia also contribute to a southward shift in rainfall associated with cyclonic synoptic waves.

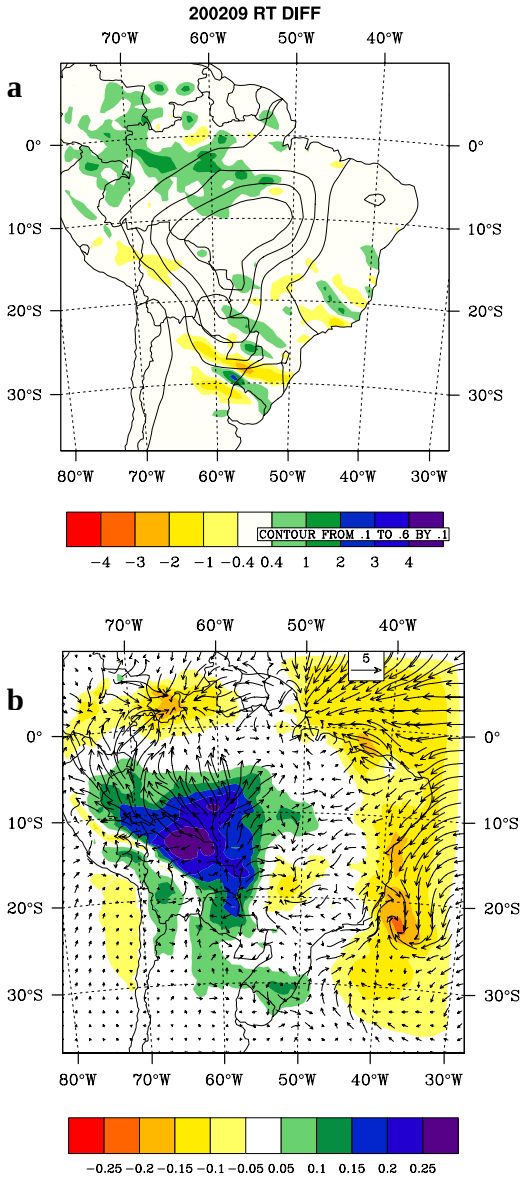

Figure 5.3.1. a) Difference of monthly mean precipitation (unit: mm) between the ensemble mean of AERO and that of the CONT simulations for September. AOD is shown by contours with interval of 0.1. b). Difference of the surface pressure (unite: hPa) and 925 hpa moisture divergence/convergence (unite: g kg^{-1} ms^{-1}) between the AERO and CONT simulations for September.

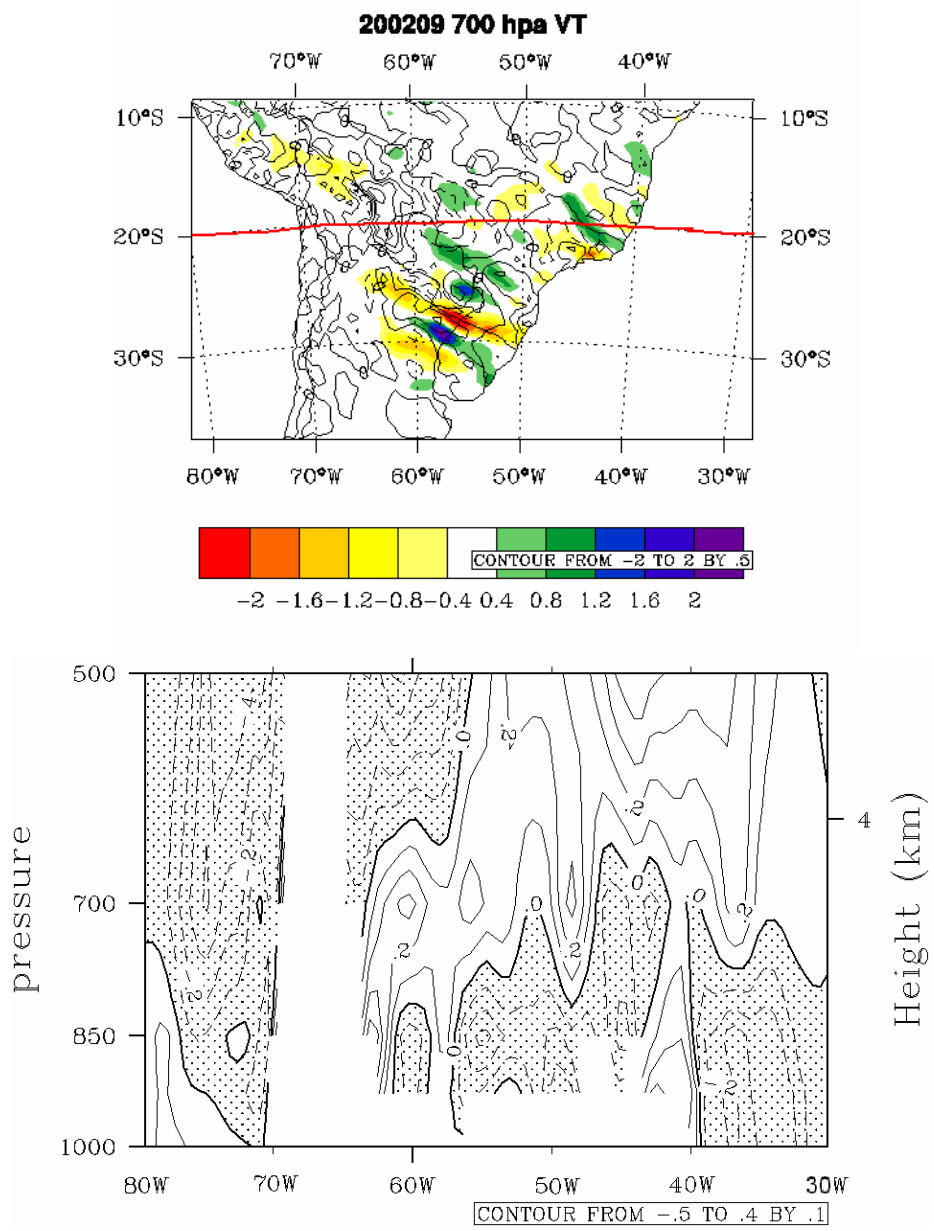

Figure 5.3.2. a) Changes of $\delta\overline{v'T'}_{700hPa}$ (contours) superimposed on the change of precipitation (shades) between ensemble mean of AERO and that of CONT in September. Solid and dashed contour represent positive or negative change of $\delta\overline{v'T'}_{700hPa}$. The red line along 20˚S indicates the geographic location of the latitude-height cross-section shown in Fig. 3b. b) Change of the meridional wind along the latitude-height cross-section at 20°S indicated in Fig. 3a. Solid contours represent positive or southerly meridional wind change and dashed contours represent negative or northerly meridional wind change. Blank area indicates the topography.

5.4 Discussion

Previous studies have established that the monsoon circulation transition from dry to wet season is initially driven by an increase of surface solar flux, which in turn increases the surface latent and sensible fluxes during September. Enhanced surface fluxes increase the surface air buoyancy and instability for moist convection, thus play a central role in initiating the monsoon transition (*Li and Fu,* 2004). The results of this study suggest that smoke aerosol radiative forcing tends to stabilize the atmosphere lapse rate in the lower troposphere in the biomass burning areas in Southern Amazonia, thus weakens the surface flux changes that initiate the monsoon transition. Such a stabilization effect increases surface pressure in Southern Amazonia, interfering with the normal southward migration of the moisture convergence center, and so causing an anomalous wind and moisture divergence in Southern Amazonia and an anomalous moisture convergence in northwestern Amazonia. Cold front incursions produce a third to a half of the rainfall in Amazonia (*Garreaud and Wallace,* 1998) and are the main mechanism to convert available potential energy into kinetic energy and spin-up the upper tropospheric anticyclonic monsoon circulation (*Krishmurti, et al.,* 1998; *Li and Fu,* 2006). Our result suggests that a more stable atmosphere due to the radiative effects of smoke aerosols in southern Amazonia may also weaken and block cold front incursions, leading to anomalously stronger synoptic perturbations and rainfall in the southeastern Brazil, Paraguay and northern Argentina. The smoke aerosol forcing also enhances the SALLJ and moisture export out of Southern Amazonia to subtropical South America. Thus, the radiative forcing of smoke aerosols appears to interfere with all three important mechanisms that drive the monsoon circulation transition in the South America. Although

the rainfall changes within the smoke center are small, the remote impacts of smoke aerosols through the dynamic response of the monsoon circulation leads to significant rainfall change outside of the smoke center, especially over northwestern Amazonia and eastern subtropical South America.

5.5 Conclusions

Simulations were carried out with the Abdus Salam Institute for Theoretical Physics Regional Climate Model (RegCM3) to test smoke aerosol radiative effect (e.g., direct and semi-direct effects) during the dry to wet transition season in Amazonia. The results suggest that the radiative forcing by smoke aerosols could interfere with the three key mechanisms that drive the monsoon circulation transition and rainfall migration to southern Amazonia.

1. An increase of surface solar flux and destabilization of the lower troposphere in southern Amazonia initiates the monsoon transition. Smoke aerosols reduce surface solar flux and stabilize the lower troposphere lapse rate in southern Amazonia where the smoke center is located.
2. Surface pressure gradient enhancement drives rapid circulation transition towards the condition needed for monsoon onset. Smoke aerosols weaken the southward surface pressure gradient and weaken the southward migration of the moisture convergence, leading to anomalous moisture divergence in southern Amazonia and anomalous moisture convergence in northwestern Amazonia.
3. Cold front incursions provide a key triggering mechanism for sudden monsoon onset. Smoke aerosols appear to block cold air incursion and increase moisture

export to the subtropical South America by stabilizing the atmosphere and increasing surface pressure in southern Amazonia.

These influences weaken the triggering mechanism for monsoon onset. Changes of circulation increase rainfall over northwestern Amazonia and eastern subtropical Amazonia outside of smoke center. Within the smoke center, the rainfall change is small presumably because the atmosphere is stable with respect to convection. Our results suggest that the dynamic response to radiative forcing by smoke aerosols has a stronger influence on rainfall change than does the local impact of aerosols during the transition period of the South America monsoon.

CHAPTER 6

CONCLUSIONS AND FUTURE WORK

We applied a regional climate model (RegCM3) to examine the direct-effect and semi-direct effect of biomass burning aerosol on land-atmospheric interaction and atmosphere circulations during the transition season from dry to wet (August – October) over Amazonia. After modification of the land scheme in RegCM3 through increasing soil layer and forest root layer depths and adding soil water to mitigate the dry bias of soil moisture in the RegCM3, we are able to significantly reduce the discrepancies between the modeled diurnal cycle of the surface sensible and latent fluxes and those observed. Smoke aerosol induced the reduction of net solar radiation in the smoke area at the surface (20 ~ 35 W m^{-2}) is mainly compensated by a reduction of surface sensible flux (15 ~ 25 W m^{-2}). Reduction of latent flux is only about 30% (5 ~ 15 W m^{-2}) of the sensible flux reduction. The diurnal cycle of surface sensible flux and latent flux are influenced by both direct radiative effect of the aerosol and cloud cover change due to aerosol absorption. A decrease of cloudiness in early afternoon partially compensates for the direct effects of smoke aerosols. This compensation changes the strongest changes of surface flux and the PBL from the noon to the late morning. Inside the smoke area, cloudiness decreases with a maximum decrease occurring in the layer right above the daytime PBL (2 km to 3 km above the surface). Outside of the smoke area in equatorial Amazonia, the cloud liquid water path increases with its maximum increase occurring below 2 km within the daytime PBL. The radiative forcing by smoke aerosols interferes with the three key mechanisms that drive the monsoon circulation transition and rainfall

migration to southern Amazonia. These influences weaken the triggering mechanism for monsoon onset and slow down the migration of rainfall intensity from northwest South America to south Amazonia, in turn, delay the monsoon onset. Our results suggest that the dynamic response to radiative forcing by smoke aerosols has a stronger influence on rainfall change over remote region than does the local impact of aerosols during the transition period of the South America monsoon.

A recent study (Takemura, et al., 2007) indicated that the simulated aerosol effect on cloud liquid water and precipitation are very different depending on whether the aerosol-atmospheric dynamic feedback mechanism is permitted in the model. This work discussed smoke aerosols radiative effect and their dynamic feedback to the atmosphere over wet to dry transition season. Next, the study of indirect effect of smoke aerosols on over this transition season will be conducted. By doing so, the aerosol acting as CCN and influence cloud amount and lifetime will be added into RegCM3 to better understand the mechanism of aerosol-monsoon interaction. Changes of cloudiness and precipitation induced by smoke aerosols will be discussed by comparing the atmospheric dynamic feedback of aerosol radiative forcing and aerosol-cloud interactions through aerosol microphysics properties. The new released RegCM3 now already includes a chemistry model. The monthly biomass burning BC and OC emission is available from Liousse. Chemistry parameters include the direct radiative effect of aerosols, the chemistry tracer name, the fraction of tracer by wet removal, and dry deposition velocities over land/ocean. So far, there is no literature published to confirm how good this chemistry model performs. Qian et al., (1999) has included a sulfur module in the RegCM2 to simulate the anthropogenic aerosols over China and their sensitivity to the parameters.

Their results show the pronounced sensitivity to prescribed dry deposition velocity. Over Amazonia, the aerosol type is quite different from China. Before the investigation of the aerosol indirect effect, similar sensitivity tests need to be done first. Then the indirect effect of biomass burning aerosol will be compared with direct effect and semi-direct effect of aerosol to estimate the total effect.

Since convective schemes in the regional model is sensitive to their parameters and regions, and smoke aerosol would influence atmospheric laps rate and static stabilities, how realistic the convective scheme presents is of importance to the study of aerosol effects. Grell (1993) convective scheme has been chosen to conduct to this study. It has some successes in simulating the patterns of precipitation over tropical South America. Unfortunately the scheme underestimates the magnitudes of both precipitation and temperature (Rauscher et al. 2006, Seth et al. 2006). RegCM3 (Pal, et al., 2007) has included a newest cumulus convection scheme (Emanuel and Zickvic Rothman 1999; Emanuel 1991) (MIT Scheme) named MIT. This scheme is more realistic compared with Grell convective scheme. It assumes that the mixing in clouds is highly episodic and inhomogeneous, and it considers convective fluxes based on an idealized model of sub-cloud-scale updrafts and downdrafts. The convection is triggered when the level of neutral buoyancy is greater than the cloud-base level. Between these two levels, air is lifted and a fraction of the condensed moisture forms precipitation while the remaining fraction forms the cloud. A comparison of RegCM3 simulation to the CAMP/CRU data demonstrated that RegCM3 using the MIT scheme performs reasonably well in simulating the distribution of precipitation over South America and its surrounding oceans during January to March (Pal et al., 2007). For the entire Amazon basin, the

simulated precipitation is within 10% of observations. So, we will conduct sensitivity tests to evaluate MIT scheme and make sure it would simulate the influence of aerosol more accurately in the transition season.

A-train satellites now provide rich information of cloud and aerosol from series of instrument of satellite, e.g., AURA, CLIPSO and CLOUDSAT. To verify the mechanism of the interaction of cloud and aerosols suggested by model simulations, we will analyze the A-Train satellite cloud and aerosol data, including aerosol loading, cloud cover, cloud type, cloud and atmospheric temperature, and relative humidity of the atmosphere with focus on South America.

APPENDIX A

AEROSOL INFLUENCE ON THE TRANSPIRATION

This section describes the perturbation of evaporation and transpiration diurnal variation due to biomass burning aerosol. The detail of formulas to calculate evaporation and transpiration could be found in BATS 1E (Dickinson et al., 1993). As we discussed in the Chapter 4, diurnal cycle of the change in evaporation and transpiration contribute to the increase of surface latent heat at noon. How transpiration changes with adjusting the stomatal resistance term in detail will be shown in this part? Figure A.1 shows the hourly perturbation of evapotranspiration (ET) from 7 to 15 LST. In the Amazon basin, ET starts to increase at 9 LST and stop increasing at 13 LST. Figure A.2 shows the transpiration perturbation without adjusting stomatal resistance. The decrease of transpiration means aerosol cooling effect. Figure A.3 shows the transpiration perturbation with adjusting stomatal resistance. When aerosol cools the surface and lower level atmosphere, transpiration increases instead of decreasing.

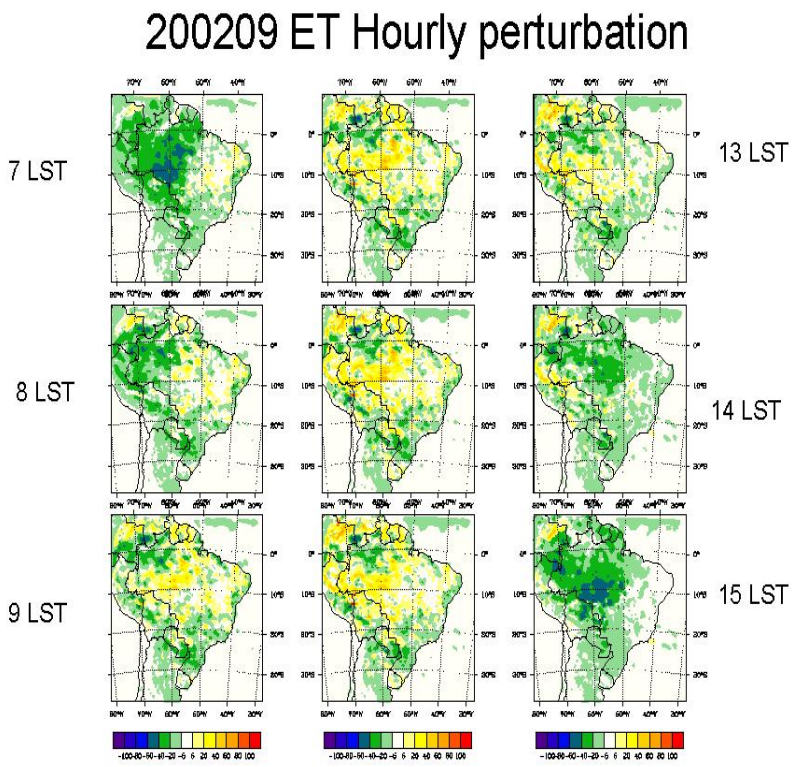

Figure A.1. Perturbation of evapotranspiratin during the day time. (Units: W m^{-2})

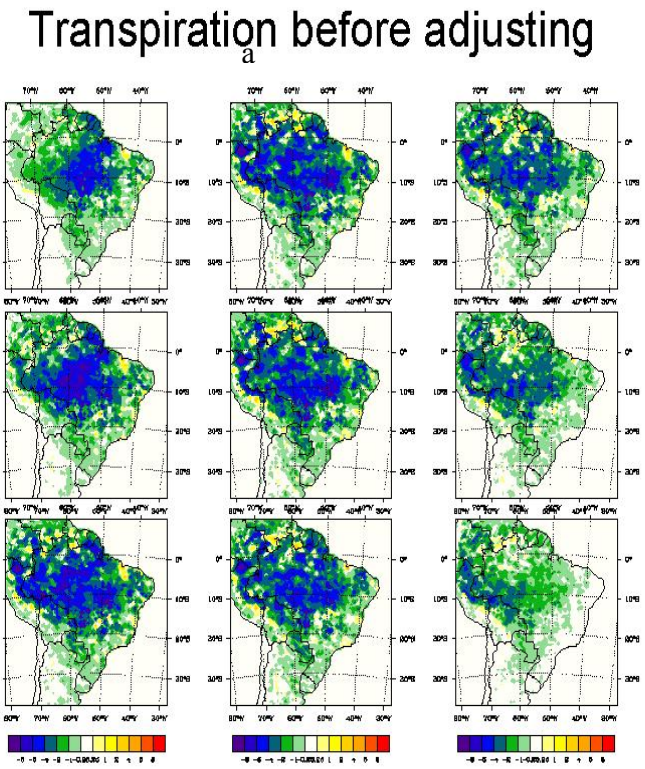

Figure A.2. Perturbation of transpiration without adjusting during the day time. (Units: W m^{-2})

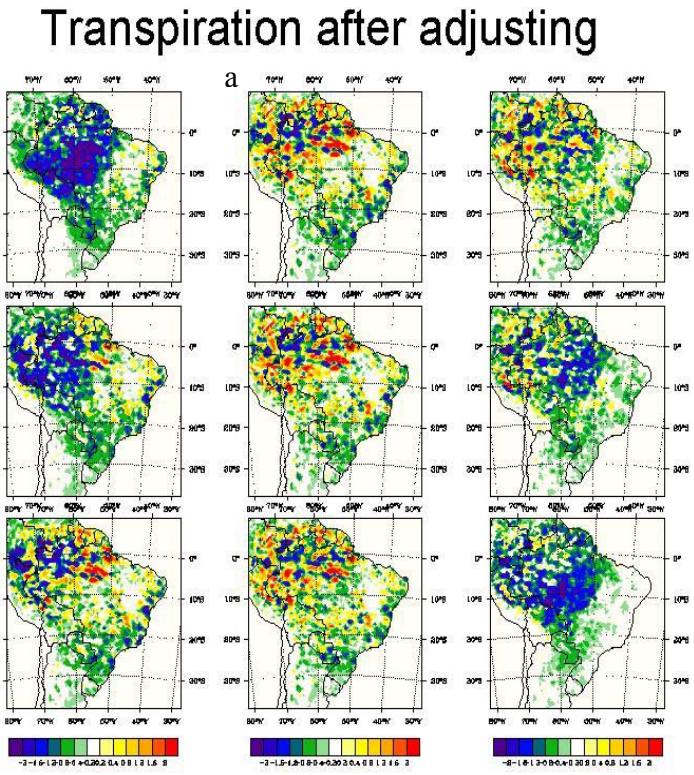

Figure A.3. Perturbation of transpiration with adjusting during the day time. (Units: W m^{-2})

REFERENCES

Aceituno, P. (1988), On the Functioning of the Southern Oscillation in the South-American Sector .1. Surface Climate, *Monthly Weather Review*, *116*, 505-524.

Ackerman, S., O. B. Toon, D. E. Stevens, A. J. Heymsfield, V. Ramanathan, and E. J.Welton (2000), Reduction of tropical cloudiness by soot, *Science, 288*, 1042–1047.

Albrecht, B. A. (1989). Aerosols, cloud microphysics, and fractional cloudiness. Science, 245, 1227−1230.

Andreae, M. O., D. Rosenfeld, P. Artaxo, A. A. Costa, G. P. Frank, K. M. Longo, and M. A. F. Silva-Diaz (2004), Smoking rain clouds over the Amazon, *Science*, 303, 1337–1341.

Andreae, M. O., et al. (1988), Biomass-Burning Emissions and Associated Haze Layers over Amazonia, *J. Geophys. Res.*, *93*, 1509-1527.

Artaxo, P., et al. (1998), Large-scale aerosol source apportionment in Amazonia, *J. Geophys. Res.*, *103*, 31837-31847.

Betts, A. K., and C. Jakob (2002), Study of diurnal cycle of convective precipitation over Amazonia using a single column model, *J. Geophys. Res., 107*(D23), 4732, doi:10.1029/2002JD002264.

Berbery, E. H., and V. R. Barros (2002), The hydrologic cycle of the La Plata basin in South America, *J. Hydrometeorology*, *3*, 630-645.

Briegleb, B. (1992), Delta-Eddington approximation for solar radiation in the NCAR community climate model, *J. Geophys. Res., 97*(D7), 7603– 7612, doi:10.1029/92JD00291.

Chand, D., P. Guyon, P. Artaxo, O. Schmid, G. P. Frank, L. V. Rizzo, O. L. Mayol-Bracero, L. V. Gatti, and M. O. Andreae (2006), Optical and physical properties of aerosols in the boundary layer and free troposphere over the Amazon Basin during the biomass burning season, *Atmos. Chem. Phys., 6*, 2911 – 2925.

Charlson, R. J. and Pilat, M. J.: Climate: The influence of aerosols, J. Appl. Meteorol., 8, 1001–1002, 1969.

Charlson, R. J., S. E. Schwartz, J. H. Hales, R. D. Cess, J. A. Coakley Jr., J. E. Hansen, and D. J. Hofmann (1992), Climate forcing by anthropogenic aerosols, *Science, 255*, 423–430.

Chin, M., P. Ginoux, S. Kinne, O. Torres, B. Holben, B. N. Duncan, R. V. Martin, J. A. Logan, A. Higurashi, and T. Nakajima (2002), Tropospheric aerosol optical thickness from the GOCART model and comparisons with satellite and Sun photometer measurements, *J. Atmos. Sci., 59*, 461–483.

Coakley Jr., J. A., Cess, R. D., and Yurevich, F. B.: The effect of tropospheric aerosols on the earth's radiation budget: A parameterization for climate models, J. Atmos. Sci., 40, 116–138, 1983.

da Rocha, H. R., M. L. Goulden, S. D. Miller, M. C. Menton, L. D. V. O. Pinto, H. C. de Freitas, and A. M. E. S. Figueira (2004), Seasonality of water and heat fluxes over a tropical forest in eastern Amazonia, *Ecol. Appl., 14*(4), S22– S32.

Dickinson, R., A. Henderson-Sellers, and P. J. Kennedy (1993), Biosphere-atmosphere transfer scheme (BATS) version le as coupled to the NCAR community climate model, *Technical Report, National Center for Atmospheric Research, Boulder, Colorado*.

Dubovik, O., B. Holben, T. Eck, A. Smirnov, Y. Kaufman,)M. King, D. Tanré, and I. Slutsker (2002), Variability of absorption and optical properties of key aerosol types observed in worldwide locations. *J. Atmos. Sci.,* 59, 590-608.

Feichter, J., E. Roeckner, U. Lohmann, and B. Liepert, 2004: Nonlinear aspects of the climate response to greenhouse gas and aerosol forcing. *J. Clim.*, **17**, 2384–2398.

Feingold, G., H. Jiang, and J. Y. Harrington (2005), On smoke suppression of clouds in Amazonia, *Geophys. Res. Lett., 32*, L02804, doi:10.1029/2004GL021369.

Fennessy, M. J., et al. (1994), The Simulated Indian Monsoon - a Gcm Sensitivity Study, *Journal of Climate*, *7*, 33-43.

Fortune, M. A., and V. E. Kousky, 1983: Two severe freezes in Brazil: Precursors and synoptic evolution. *Mon. Wea. Rev.,* **111,** 181– 196.

Freitas, S. R., K. M. Longo, et al., 1997, Numerical modeling of air mass trajectories from the biomass burning areas of the Amazon basin. Annais da Academia Brasileira de Ciencias 68: 193-206

Fu, R., B. Zhu, and R. E. Dickinson (1999), How do the atmosphere and land surface influence seasonal changes of convection in the tropical Amazon?, *J. Clim., 12*, 1306– 1321.

Fu, R., R. E. Dickinson, M. X. Chen, and H. Wang, 2001: How do tropical sea surface temperatures influence the seasonal distribution of precipitation in the equatorial Amazon, *J. Climate*, **14**, 4003-4026.

Garreaud, R. D., and J. M. Wallace (1998), Summertime incursions of midlatitude air into subtropical and tropical South America, *Mon. Weather Rev.*, *126*, 2713-2733.

Garreaud, R. D. (1999), Cold air incursions over subtropical and tropical South America: A numerical case study, *Mon. Weather Rev.*, *127*, 2823-2853.

Gash, J. H. C., and C. A. Nobre (1997), Climatic effect of Amazonian deforestation: Some results from ABRACOS, *Bull. Am. Meteorol. Soc., 78*, 823– 830.

Ghan, S.J., G. Guzman, and H. Abdul-Razzak, 1998: Competition between sea salt and sulphate particles as cloud condensation nuclei. *J. Atmos. Sci.*, **55**, 3340–3347.

Goulden, M. L., S. D. Miller, H. R. da Rocha, M. C. Menton, H. C. de Freitas, A. M. E. S. Figueira, and C. A. D. de Sousa (2004), Diel and seasonal patterns of tropical forest CO2 exchange, *Ecol. Appl., 14*(4), S42– S54.

Grell, G. A. (1993), Prognostic evaluation of assumptions used by cumulus parameterizations, *Mon. Weather Rev., 121*, 764–787.

Grell, G. A., J. Dudhia, and D. R. Stauffer (1994), A description of the fifth-generation Penn State/NCAR mesoscale model (MM5), *NCAR Tech. Note TN-398+STR*, 122 pp., Natl. Cent. for Atmos. Res., Boulder, Colo.

Grimm, A. M., et al. (2007), Connection between spring conditions and peak summer monsoon rainfall in South America: Role of soil moisture, surface temperature, and topography in eastern Brazil, *Journal of Climate*, *20*, 5929-5945.

Gutman, G.J., and W. Schwerdtfeger, 1965: The role of latent and sensible heat for the development of a high-pressure system over the subtropical Andes in the summer. *Metero. Rundsch.,* 18, 69-76

Hamilton, M. G., and J. R. Tarifa (1978), Synoptic Aspects of a Polar Outbreak Leading to Frost in Tropical Brazil, July 1972, *Monthly Weather Review*, *106*, 1545-1556.

Hansen, JE, AA Lacis (1990), Sun and dust versus greenhouse gases: an assessment of their relative roles in global climate change. Nature 346: 713-718

Hansen, JE, M. Sato, and R. Ruedy (1997), Radiative forcing and climate response. *J. Geophys. Res., 102*, 6831– 6864.

Hansen, J, and L. Nazarenko, (2004), Soot climate forcing via snow and ice albedos, *Pro. Natl. Acad. Sci.* U. S. A., 101, 423-428

Haywood, J. and Boucher, O.: Estimates of the direct and indirect radiative forcing due to tropospheric aerosols: A review, Rev. Geophys., 38, 513–543, 2000.

Hobbs, P. V., et al. (1997), Direct radiative forcing by smoke from biomass burning. *Science*, *275*, 1776-1778.

Hoskins, B. J., and P. J. Valdes (1990), On the Existence of Storm-Tracks, *J. Atmos. Sciences*, *47*, 1854-1864.

Horel, J. D., et al. (1989), An Investigation of the Annual Cycle of Convective Activity over the Tropical Americas, *J. Clim.*, *2*, 1388-1403.

Huang, Y., R. E. Dickinson, and W. L. Chameides (2006), Impact of aerosol indirect effect on surface temperature over east Asia, *Proc. Natl. Acad. Sci. U. S. A., 103*, 4371– 4376, doi:10.1073/pnas.0504428103.

Jacobson, M.Z., 2001b: Strong radiative heating due to the mixing state of black carbon in atmospheric aerosols. *Nature*, **409**, 695–697.

Johnson, B. T., K. P. Shine, and P. M. Forster (2004), The semi-direct aerosol effect: Impact of absorbing aerosols on marine stratocumulus, *Q. J. R. Meteorol. Soc., 130*, 1407–1422.

Jones, A., D.L. Roberts, and M.J. Woodage, 2001: Indirect sulphate aerosol forcing in a climate model with an interactive sulphur cycle. *J. Geophys. Res*., **106**(D17), 20293–20301.

Kaufman, Y. J., A. Setzer, D. Ward, D. Tanre, B. N. Holben, P. Menzel, M. C. Pereira, and R. Rasmussen (1992), Biomass burning airborn and spaceborne experiment in the Amazons (BASE-A), *J. Geophys. Res., 97,* 14,581–14,599.

Kaufman, Y. J., et al. (1998), Smoke, Clouds, and Radiation – Brazil (SCAR-B) experiment, *J. Geophys. Res., 103*, 31,783– 31,808.

Kaufman Y.J., et al., 2005a: Aerosol anthropogenic component estimated from satellite data. *Geophys. Res. Lett*., **32**, L17804, doi:10.1029/2005GL023125.

Kaufman, Y. J., and I. Koren (2006), Smoke and pollution aerosol effect on cloud cover, *Science, 313*, 655– 658.

Kiehl, J. T., J. J. Hack, G. B. Bonan, B. A. Boville, D. L. Williamson, and P. J. Rasch (1998), The National Center for Atmospheric Research Community Climate Model: CCM3, *J. Clim., 11*, 1131– 1150.

Kleidon, A., and M. Heimann (2000), Assessing the role of deep rooted vegetation in the climate system with model simulations: Mechanism, comparison to observations and implications for Amazonian deforestation, *Clim. Dyn., 16*, 183– 199.

Kodama, Y. M., and A. Tamaoki (2002), A re-examination of precipitation activity in the subtropics and the mid-latitudes based on satellite-derived data, *Journal of the Meteorological Society of Japan*, *80*, 1261-1278.

Koren, I., Y. J. Kaufman, L. A. Remer, and J. V. Martins (2004), Measurement of the effect of Amazon smoke on inhibition of cloud formation, *Science, 303*, 1342–1345.

Koren, I., et al. (2007), Reversal of trend of biomass burning in the Amazon, *Geophysical Research Letters*, *34*.

Kousky, V. E., 1988: Pentad outgoing longwave radiation climatology for the South American sector. *Rev. Brasil. Meteor.,* 3, 217–231.

Krishnamurti, T. N., et al. (1998), A study of south Asian monsoon energetics, *J. Atmos. Sci.,*, *55*, 2530-2548.

Libmann, B.; G. Kiladis, J. Marengo, T. Ambrizzi, and J. D. Glick, 1999: Submonthly convective variability over South America and the South Atlantic convergence zone. *J. Climate,* **12,** 1877–1891.

Landulfo, E., et al. (2003), Synergetic measurements of aerosols over Sao Paulo, Brazil using LIDAR, sunphotometer and satellite data during the dry season, *Atmos. Chem. Phys*, *3*, 1523-1539.

Labonne, M., F. M. Bréon, and F. Chevallier (2007), Injection height of biomass burning aerosols as seen from a spaceborne lidar, *Geophys. Res. Lett,34*(11), L11806, doi:10.1029/2007GL029311.

Lau, K.-M., et al., 2008: The joint Aerosol-Monsoon experiment. Bull. Am. Meteorol. Soc., 89(3), 369-383.

Lenters, J. D., and K. H. Cook (1999), Summertime precipitation variability over South America: Role of the large-scale circulation, *Monthly Weather Review*, *127*, 409-431.

Liepert, B.G., J. Feichter, U. Lohmann, and E. Roeckner, 2004: Can aerosols spin down the water cycle in a warmer and moister world. *Geophys. Res. Lett.*, **31**, L06207, doi:10.1029/2003GL019060.

Lohmann, U., and J. Feichter, 2001: Can the direct and semi-direct aerosol effect compete with the indirect effect on a global scale? *Geophys. Res. Lett.*, **28**(1), 159–161, doi:10.1029/2000GL012051.

Lohmann, U., and J. Feichter, 2005: Global indirect aerosol effects: A review. *Atmos. Chem. Phys.*, **5**, 715–737.

Lohmann, U., I. Koren, and Y.J. Kaufman, 2006: Disentangling the role of microphysical and dynamical effects in determining cloud properties over the Atlantic. *Geophys. Res. Lett.*, **33,** L09802, doi:10.1029/2005GL024625.

Li, W. H., and R. Fu (2004), Transition of the large-scale atmospheric and land surface conditions from the dry to the wet season over Amazonia as diagnosed by the ECMWF re-analysis, *J. Clim.*, *17*, 2637-2651.

Li, W. H., and R. Fu (2006), Influence of Cold Air Intrusions on the Wet Season Onset over Amazonia, *J. Clim.*, **19**, 257-275.

Liebmann, B., et al. (1998), A comparison of rainfall, outgoing longwave radiation, and divergence over the Amazon Basin, *J. Clim.*, *11*, 2898-2909.

Liu, Y. Q. (2005), Atmospheric response and feedback to radiative forcing from biomass burning in tropical South America, *Agri. Forest Meteoro*, *133*, 40-53.

Malhi, Y., E. Pegoraro, A. D. Nobre, M. G. P. Pereira, J. Grace, A. D. Culf, and R. Clement (2002), Energy and water dynamics of a central Amazonian rain forest, *J. Geophys. Res., 107*(D20), 8061, doi:10.1029/2001JD000623.

Marengo, J., A. Cornejo, P. Satymurty, C. Nobre, and W. Sea, 1997: Cold surges in tropical and extratropical South America: The strong event in June 1994. *Mon. Wea. Rev.,* **125,** 2759–2786.

Marengo, J. A. (2004), Interdecadal variability and trends of rainfall across the Amazon basin, *Theoretical and Applied Climatology*, *78*, 79-96.

Marengo, J. A., et al. (2001), Onset and end of the rainy season in the Brazilian Amazon Basin, *J. Clim.*, *14*, 833-852.

McCormick, R. A. and Ludwig, J. H.: Climate modification by atmospheric aerosols, Science, 156(3780), 1358–1359, 1967.

Menon, S., J. Hansen, L. Nazarenko, and Y. Luo (2002), Climate effects of black carbon aerosols in China and India, *Science, 297*, 2250 - 2253.

Menon, S., et al., 2003: Evaluating aerosol/cloud/radiation process parametrizations with single-column models and Second Aerosol Characterization Experiment (ACE-2) cloudy column observations. *J. Geophys. Res.*, **108**(D24), 4762, doi:10.1029/2003JD003902.

Myhre, G., and A. Myhre, 2003: Uncertainties in radiative forcing due to surface albedo changes caused by land-use changes. *J. Clim.*, **16**, 1511– 1524.

Nakamura, H., et al. (2002), Interannual and decadal modulations recently observed in the Pacific storm track activity and east Asian winter monsoon, *J. Clim.*, *15*, 1855-1874.

Namias, J. (1972), Space Scales of Sea-Surface Temperature Patterns and Their Causes, *Fishery Bulletin of the National Oceanic and Atmospheric Administration*, *70*, 611-617.

Nobre, P., G. Fisch, H. R. da Rocha, R. F. F. Lyra, E. P. da Rocha, and V. N. Ubarana, 1996: Observation of the atmospheric boundary layer in Rondônia, Amazonian Deforestation and Climate, J. H. C. Gash, C. A. Nobre, J. M. Robert, and R. L. Victoria, Eds., John Wiley, 413-424.

Nepstad, D. C., et al. (1994), The role of deep roots in the hydrological and carbon cycles of Amazonian forests and pastures, *Nature, 372*, 666– 669.

Pal, J. S., et al. (2007), Regional climate modeling for the developing world - The ICTP RegCM3 and RegCNET, *Bull. Am. Meteorol. Soc., 88*, 1395-+.

Pathirana, A., et al. (2007), Impacts of absorbing aerosols on South Asian rainfall - A modeling study, *Climatic Change*, *85*, 103-118.

Penner, J. E., et al. (1992), Effects of Aerosol from Biomass Burning on the Global Radiation Budget, *Science*, *256*, 1432-1434.

Penner, J., et al., 2001: Aerosols, their direct and indirect effects. In: *Climate Change 2001: The Scientifi c Basis. Contribution of Working Group I to the Third Assessment Report of the Intergovernmental Panel on Climate Change* [Houghton, J.T., et al. (eds.)]. Cambridge University Press, Cambridge, United Kingdom and New York, NY, USA, pp. 289–348.

Penner, J.E., S.Y. Zhang, and C.C. Chuang, 2003: Soot and smoke aerosol may not warm climate. *J. Geophys. Res.*, **108**(D21), 4657, doi:10.1029/2003JD003409.

Penner, J.E., et al., 2006: Model intercomparison of indirect aerosol effects. *Atmos. Chem. Phys. Discuss.*, **6**, 1579–1617.

Petersen, W. A., et al. (2002), TRMM observations of intraseasonal variability in convective regimes over the Amazon, *Journal of Climate*, *15*, 1278-1294.

Procopio, A. S., P. Artaxo, Y. J. Kaufman, L. A. Remer, J. S. Schafer, and B. N. Holben (2004), Multiyear analysis of Amazonian biomass burning smoke radiative forcing of climate, Geophys. *Res. Lett., 31*, L03108, doi:10.1029/2003GL018646.

Qian, Y., and F. Giorgi (1999), Interactive coupling of regional climate and sulfate aerosol models over eastern Asia, *J. Geophys. Res*, *104*, 6477-6499.

Reid, J., T. Eck, S. Christopher, R. Koppmann, O. Dubovik, D. Eleuterio, B. Holben, E. Reid, and J. Zhang (2005): A review of biomass burning emissions part III: intensive optical properties of biomass bunring particles, *Atmos. Chem. Phys*., 5, 827-849.

Rao, G. V., and S. Erdogan (1989), The Atmospheric Heat-Source over the Bolivian Plateau for a Mean January, *Boundary-Layer Meteorology*, *46*, 13-33.

Rao, V. B., et al. (1996), Annual variation of rainfall over Brazil and water vapor characteristics over South America, *Journal of Geophysical Research-Atmospheres*, *101*, 26539-26551.

Ramanathan, V., P.J. Crutzen, J.T. Kiehl, and D. Rosenfeld, 2001: Atmosphere: aerosols, climate, and the hydrological cycle. *Science*, **294**, 2119–2124.

Ramanathan, V., et al., 2005: Atmospheric brown clouds: impacts on South Asian climate and hydrological cycle. *Proc. Natl. Acad. Sci. U.S.A.*, **102**, 5326–5333.

Ramaswamy, V., et al., 2001: Radiative forcing of climate change. In: *Climate Change 2001: The Scientifi c Basis. Contribution of Working Group I to the Third Assessment Report of the Intergovernmental Panel on Climate Change* [Houghton, J.T., et al. (eds.)]. Cambridge University Press, Cambridge, United Kingdom and New York, NY, USA, pp. 349–416.

Rauscher S. A., A. Seth A, B. Liebmann, J. Qian, and S. J. Camargo (2007): Regional climate model - Simulated timing and character of seasonal rains in South America. *Mon. Weather Rev* 135 (7): 2642-2657

Rickenbach, T. M., et al. (2002), Modulation of convection in the southwestern Amazon basin by extratropical stationary fronts, *J. Geophys. Res.*, *107*. doi: 10.1029/2000JD000263

Rosenfeld, D. (1999), TRMM observed first direct evidence of smoke from forest fires inhibiting rainfall, *Geophys. Res. Lett.*, *26*, 3105-3108.

Schafer, J. S., et al. (2008), Characterization of the optical properties of atmospheric aerosols in Amazonia from long-term AERONET monitoring (1993-1995 and 1999-2006), *Journal of Geophysical Research-Atmospheres*, *113*.

Seth, A., and F. Giorgi (1998), The effects of domain choice on summer precipitation simulation and sensitivity in a regional climate model, *J. Clim.*, *11*, 2698-2712.

Smirnov, A., B. N. Holben, T. F. Eck, I. Slutsker, B. Chatenet, and R. T. Pinker (2002), Diurnal variability of aerosol optical depth observed at AERONET (Aerosol Robotic Network) sites, *Geophys. Res. Lett., 29*(23), 2115, doi:10.1029/2002GL016305.

Steiner, A. L., and W. L. Chameides (2005), Aerosol-induced thermal effects increase modelled terrestrial photosynthesis and transpiration, *Tellus Series B-Chemical and Physical Meteorology*, *57*, 404-411.

Torrence, C., and P. J. Webster (1998), The annual cycle of persistence in the El Nino Southern Oscillation, *Quarterly Journal of the Royal Meteorological Society*, *124*, 1985-2004.

Twomey, S. (1977), The influence of pollution on the shortwave albedo of clouds, *J. Atmos. Sci., 34*, 1149– 1152..

Vera, C., et al. (2006), The South American low-level jet experiment, *Bulletin of the American Meteorological Society*, *87*, 63-77.

Vera, C., et al. (2006), Toward a unified view of the American Monsoon Systems, *Journal of Climate*, *19*, 4977-5000.

von Randow, C., et al. (2004), Comparative measurements and seasonal variations in energy and carbon exchange over forest and pasture in South West Amazonia, *Theor. Appl. Climatol., 78*, 5 – 26.

Wang, C., 2004: A modeling study on the climate impacts of black carbon aerosols. *J. Geophys. Res.*, **109**, doi:10.1029/2003JD004084.

Wang, H., and R. Fu, 2002: Cross-equatorial flow and seasonal cycle of precipitation over South America. *J. Clim.*, **15,** 1591–1608.

Webster, P. J., et al. (1998), Monsoons: Processes, predictability, and the prospects for prediction, *Journal of Geophysical Research-Oceans*, *103*, 14451-14510.

Williams, E., and N. Renno (1993), An analysis of the conditional instability of the tropical atmosphere, *Mon. Weather Rev.*, *121*, 21-36.

Xie, P. P., and P. A. Arkin (1997), Global precipitation: A 17-year monthly analysis based on gauge observations, satellite estimates, and numerical model outputs, *Bull. Am. Meteorol. Soc.*, *78*, 2539-2558.

Xue, Y. K., and J. Shukla (1993), The Influence of Land-Surface Properties on Sahel Climate .1. Desertification, *Journal of Climate*, *6*, 2232-2245.

Yu, H., S. C. Liu, and R. E. Dickinson (2002), Radiative effects of aerosols on the evolution of the atmospheric boundary layer, *J. Geophys. Res., 107*, 4142, doi:10.1029/2001JD000754.

Yu, H., R. E. Dickinson, M. Chin, Y. J. Kaufman, B. N. Holben, I. V. Geogdzhayev, and M. I. Mishchenko (2003), Annual cycle of global distributions of aerosol optical depth from integration of MODIS retrievals and GOCART model simulations, *J. Geophys. Res., 108*, 4128, doi:10.1029/2002JD002717.

Yu, H., et al. (2006), A review of measurement-based assessment of aerosol direct radiative effect and forcing, *Atmos. Chem. Phys., 6*, 613– 666.

Yu, H., R. Fu, R. E. Dickinson, Y. Zhang, M. Chen, and H. Wang (2007), Interannual variability of smoke and warm cloud relationships in the Amazon as inferred from MODIS retrievals. *Remote Sens. Environ.*, doi:10.1016/j.rse.2007.04.003.

Zhou, M., H. Yu, R. E. Dickinson, O. Dubovik, and B. N. Holben (2005), A normalized description of the direct effect of key aerosols types on solar radiation as estimated from AERONET aerosols and MODIS albedos, *J. Geophys. Res., 110*, D19202, doi:10.1029/2005JD005909.

Zhou, J. Y., and K. M. Lau (1998), Does a monsoon climate exist over South America?, *Journal of Climate*, *11*, 1020-1040.

Zhang, Y., R. Fu, H. Yu, R. E. Dickinson, R N. Juarez, M. Chin, and H. Wang (2008), A regional climate model study of how biomass burning aerosol impacts land-atmosphere interactions over the Amazon, *J. Geophys. Res.*, *113*, D14S15, doi:10.1029/2007JD009449.